processes

Review

Fundamentals and Manipulation of Bare Droplets and Liquid Marbles as Open Microfluidic Platforms

Zheng Huang [1,2], Yuanhao Xie [1,2], Huaying Chen [1], Zhihang Yu [2], Liuyong Shi [3] and Jing Jin [1,*]

[1] School of Mechanical Engineering and Automation, Harbin Institute of Technology, Shenzen, Shenzhen 518055, China
[2] School of Science, Harbin Institute of Technology, Shenzhen, Shenzhen 518055, China
[3] Mechanical and Electrical Engineering College, Hainan University, Haikou 570228, China
* Correspondence: jinjing2020@hit.edu.cn

Abstract: Microfluidics, as one of the most valuable analytical technologies of this century, has played an important role in various fields. Particularly, out-of-channel microfluidics, often referred to as open microfluidics (OMF) has recently drawn wide research attention among scholars for its great potential in convenient manual intervention. Much recent research has been geared toward bare droplets and particle-armed droplets (namely liquid marbles, LMs), which could serve as independent systems in OMF. Their versatile applications include but are not limited to nanomaterials preparation, energy harvesting, cell culture and environment monitoring. These applications are mainly attributed to the excellent independence, low reagent consumption and short reaction time of separate droplets and LMs. In addition, more operation features, such as diverse handling options, flexible controllability and high precision, further enable droplets and LMs carrying small liquid biochemical samples to be manipulated in an open environment freely. Considering the emergence of important research on bare droplets and LMs, this paper systematically reviews the state of the art in the fundamentals and manipulation of the two novel platforms under the frame of OMF. First, the intrinsic property of bare droplets on solid substrates, especially on superhydrophobic ones, is discussed, followed by the formation mechanism of nonwetting LMs and the effect of coating particles on LMs' performance. Then, friction obstacles and actuation principles raised in driving droplets and LMs are further analyzed theoretically. Subsequently, several classical types of manipulation tasks for both droplets and LMs, namely transportation, coalescence, mixing and splitting, are discussed with a focus on key techniques to accomplish the tasks aforementioned. Finally, the fundamental and manipulation similarities and differences between bare droplets and LMs are summarized and future developments towards droplet- or LM-based microreactors and microsensors are recommended accordingly.

Keywords: droplets; liquid marbles; open microfluidics; manipulation; hydrodynamics

Citation: Huang, Z.; Xie, Y.; Chen, H.; Yu, Z.; Shi, L.; Jin, J. Fundamentals and Manipulation of Bare Droplets and Liquid Marbles as Open Microfluidic Platforms. *Processes* **2023**, *11*, 983. https://doi.org/10.3390/pr11040983

Academic Editor: Rui A. Lima

Received: 15 February 2023
Revised: 16 March 2023
Accepted: 19 March 2023
Published: 23 March 2023

1. Introduction

Miniaturization has become one of the dominant themes in the fields of chips, micro electromechanical systems (MEMS) and other electronic components. As a prominent example of MEMS extension, microfluidic platforms are no exception and have been developing towards miniaturization in the past decades [1]. By definition, microfluidics aims to manipulate limited fluids at the microscopic scale, where the effect of surface tension is much greater than that of gravity and could thus be adopted in various manipulation tasks [2–6]. The microscale nature of microfluidics features numerous advantages, such as tiny device size, low reagent consumption and short reaction time. These advantages render microfluidic platforms, especially droplet microfluidic platforms, excellent miniaturized reactors or sensors with much more controllable conditions. This demonstrates great inventiveness and superiority in biochemical analysis and micro-/nano-fabrication that are incomparable to traditional technologies [7–12].

While conventional microfluidics operates small volumes of fluid within closed channels, open microfluidics (OMF), as its name indicates, manipulates fluids freely in an open environment [12,13]. Here fluids, especially discrete liquids, interact with the external environment partially or absolutely. This breaks the barrier of enclosed space in which fluids are stored and provides more operational possibilities. As independent functional platforms in OMF, bare droplets and liquid marbles (LMs), namely sessile pure droplets and core–shell droplet systems respectively, possess many unique features besides the inherent advantages of conventional droplet microfluidics [14]. Droplets on a solid surface are usually directly exposed to air and isolated by the liquid–air interface, which means that there is a flexible operating room allowing for convenient surface modification. For example, reagents can be arbitrarily added into bare droplets and products can be easily removed reversely [15]. Furthermore, bare droplets on a superhydrophobic surface keep sphere shapes, which offers a microscale 3D liquid interior space. Based on the above features, droplets in OMF have excellent performance in cell culture, materials synthesis, biochemical analysis, and clinical therapies [16–20]. Unfortunately, the vast liquid–air surface of droplets also poses some problems. Here liquids are more susceptible to external contamination and may evaporate rapidly, resulting in a short lifecycle. By contrast, an LM, which is a bare droplet encapsulated by multilayered hydrophobic particles, could effectively reduce the evaporation rate of the core liquid and provide an isolated environment under the protection of the particle shell, allowing for sufficient running time in operation [21,22].

In addition, compared with bare droplets, LMs exhibit the features of high stability, good elasticity, low friction and reliable three-phase contact, offering more options for liquid handling [23,24]. For example, LMs can be manipulated on a liquid surface or even inside carrier liquid, greatly expanding the use scope of droplet systems [25–27]. Meanwhile, the transition between the stable state and the collapsed state of a particle shell gives LMs the information transfer capacity. Thus, they can serve as various microsensors on certain occasions for gas sensing, water surface contaminant detection and water system remediation [28–30]. However, LMs also have some undesired drawbacks such as low environmental sensitivity and complicated intervention steps, due to the overprotection of the multilayered particle shell. Despite this, droplets and LMs are still important and complementary microsystems from life sciences to industrial applications, significantly promoting the development of OMF and further droplet microfluidics.

This paper reviews recent studies on bare droplets and LMs, from fundamental features to manipulation techniques, as schematically shown in Figure 1. First, it discusses the fundamentals of droplets and LMs, including the intrinsic property of droplets on a solid surface, the mechanism of LM formation, and the particulate factor that affects the performance of LMs. Subsequently, it presents the friction obstacles of droplets and LMs that have to be overcome in actuating on different carrier substrates and classifies the general actuation principles for effective liquid manipulation. A comprehensive understanding of the properties of droplets and LMs lays the basis for further discussion on efficient operations. Later, several manipulation tasks of droplets and LMs are respectively discussed, including transportation, coalescence, mixing and splitting. Then, representative techniques used for manipulation are presented, and the characteristics exhibited by bare droplets and LMs in handling processes are analyzed and compared. Finally, the similarities and differences between droplets and LMs in fundamentals as well as operations are briefly summarized, and future research directions towards these two emerging OMF platforms are outlined based on the above discussion.

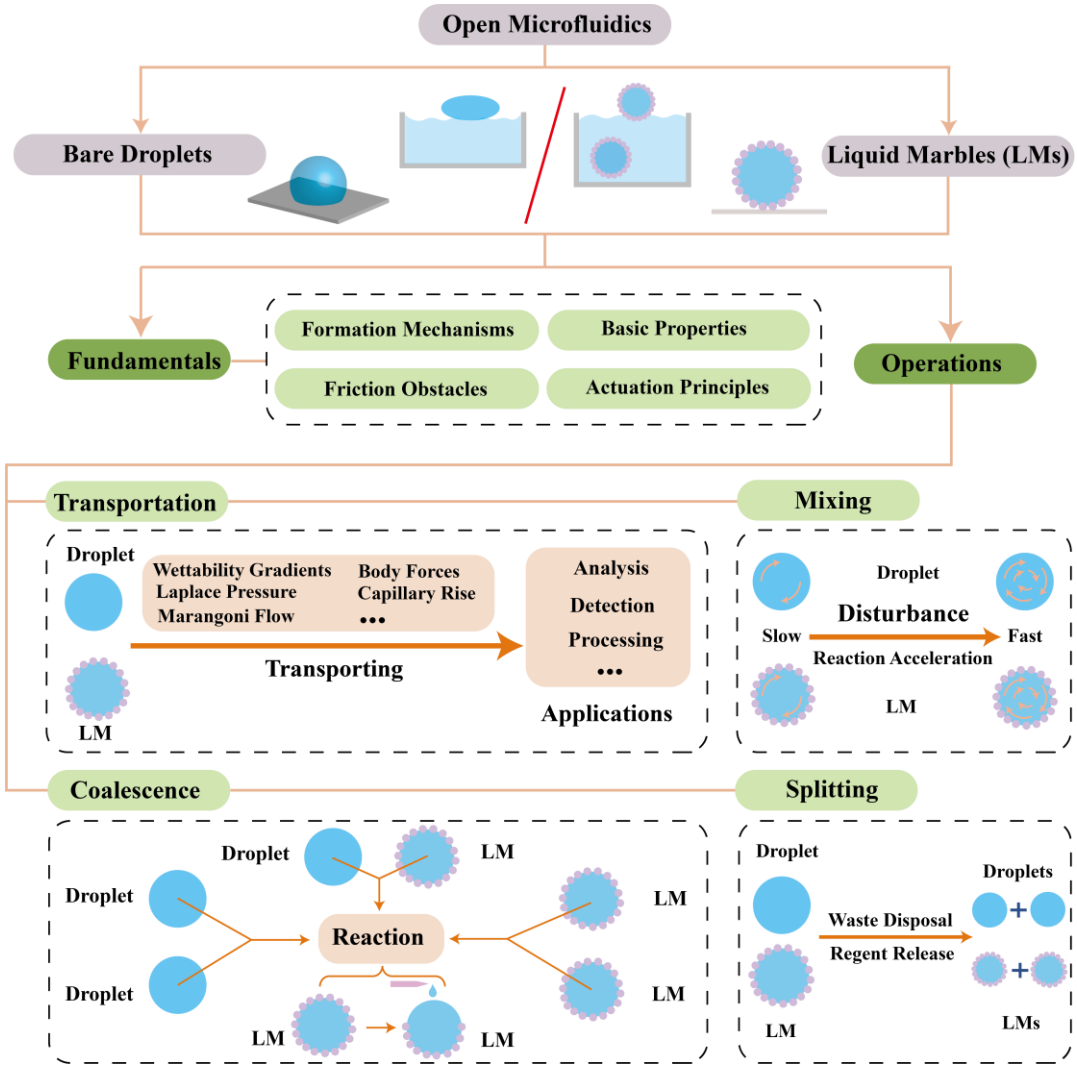

Figure 1. The research strategy for fundamentals and operations of bare droplets and LMs in OMF. The discussion on the fundamentals of bare droplets and LMs mainly involves their formation mechanisms, basic properties, friction obstacles and actuation principles. The operation tasks of droplets and LMs can be divided into four types based on specific functions: transportation for transferring objects simply, coalescence for merging two isolated samples, mixing for blending different contents in reactions and splitting for cutting an origin sample into multi-samples.

2. Fundamentals of Bare Droplets and Liquid Marbles

2.1. Bare Droplets on Solid Substrates

A droplet is a tiny volume of liquid isolated by a liquid–air interface and ubiquitous in nature. For example, thousands of free raindrops falling from the sky can rest on various substrates and turn to the sessile status. On a concrete surface, droplets look floppy. However, when on a solid surface such as plant leaves, they behave pretty firmly. These unusual dynamic behaviors of droplets on a solid surface endow them with a wide range of potential applications with enormous advantages and have attracted the attention of interdisciplinary researchers. In recent years, research on bare droplets on a solid surface has investigated its functions in terms of handling small amounts of liquid samples, harvesting low-grade energy sources, manufacturing functional materials, and sensing chemical and biological analytes [31]. In order to understand the mechanism behind these related applications, learning more details about droplets on a solid surface is necessary, especially on a superhydrophobic surface.

Theoretically, droplets often have three wetting states on a solid surface: completely wet, partially wet and completely dry, Figure 2a. In most cases, droplets on a solid surface stay in the partially wet state. The three states are the reasonable result of surface tensions among solid/liquid/gas phases, and these states are expressed macroscopically as a difference in the magnitude of the equilibrium contact angle θ_{eq} [32]. Based on the contact angle of a droplet on solids, solid surfaces can be further classified into hydrophilic and hydrophobic types roughly, Figure 2b. When $0^{\circ} < \theta_{eq} < 90^{\circ}$, a surface is hydrophilic, while $90^{\circ} < \theta_{eq} < 180^{\circ}$, the surface tends to be hydrophobic. Particularly, for $\theta_{eq} \geq 150^{\circ}$, this surface can be defined as superhydrophobic, which is preferred and often adopted in manipulating bare droplets.

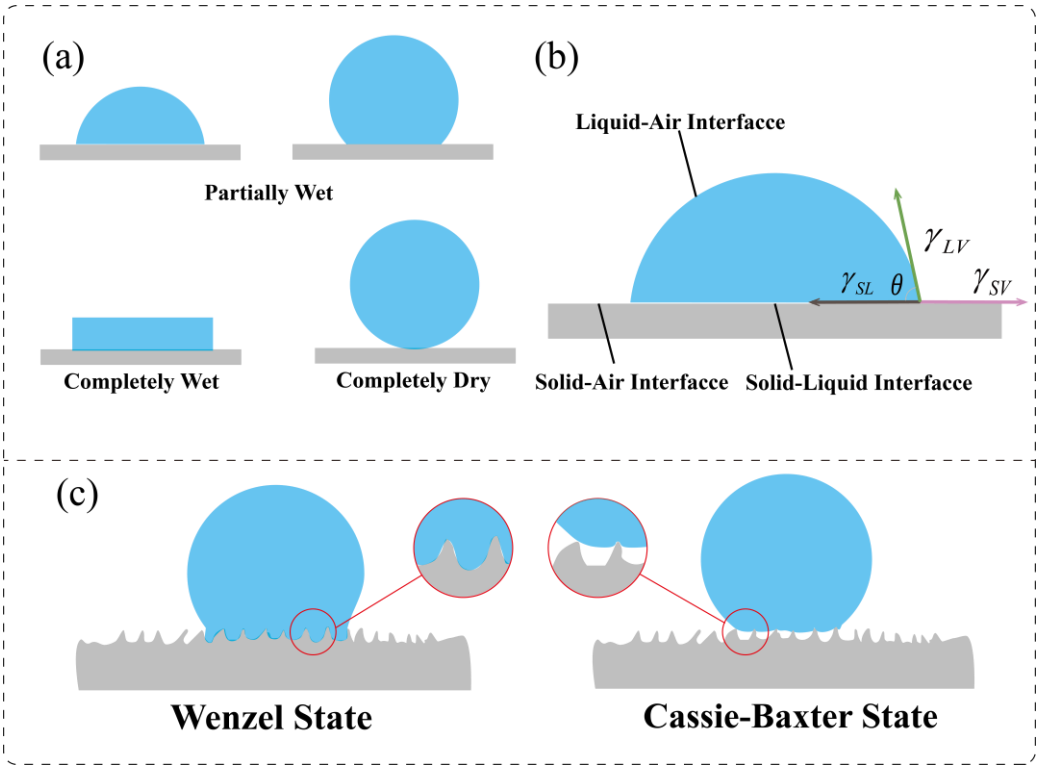

Figure 2. (**a**) Different wetting states of droplets resting on solid substrates. (**b**) Conceptual diagram of three-phase contact angle. (**c**) Two common states of droplets on a topologically patterned surface.

In nature, there are various superhydrophobic surfaces, such as lotus leaves, rice leaves, and Brassica oleracea leaves. On these natural surfaces, droplets behave like balls that can be easily actuated [33]. In addition to the inherent hydrophobicity, some plant surfaces also show distinctive properties and behaviors. For example, rice leaves could transport droplets on their surface unidirectionally and hogweeds may even transport droplets against gravity [34,35]. By studying the superhydrophobicity exhibited by plants, it is found that higher hydrophobicity is congruent with rougher solid surfaces [36,37]. Inspired by these plant surfaces, many superhydrophobic surfaces with similar structures have been created artificially and applied in surface self-cleaning and anti-icing [38,39]. Moreover, by figuring out the mechanisms behind extraordinary droplet transportation phenomena in nature, the potential application of water droplets on superhydrophobic surfaces has been successfully demonstrated, such as 3D cell culture, blood type testing and detection of multiple analytes from a single sample [16,19,40].

Superhydrophobic surfaces of plants have a large number of microstructures. Due to the microstructures, the actual surface area is much larger than its geometrical surface area, especially the superhydrophobic surface with many pre-designed microstructures. It means that the actual surface energy is higher than the geometrical surface energy. At the same time, on these surfaces, the equilibrium state of a droplet changes and can be

divided into two opposite states, namely the Wenzel state and the Cassie–Baxter state, Figure 2c. In the Wenzel state, droplets completely pass through the space between the surface pillars, while in the Cassie–Baxter state, the droplet stays on top of the surface pillars [41]. The calculation of the contact angle in both states generally requires a certain degree of correction according to the detailed surface microstructures. The apparent contact angle of a droplet in the Wenzel state and the Cassie–Baxter state can be represented by θ_w and θ_D respectively and calculated as [42,43]:

$$cos\theta_w = rcos\theta_{eq} \quad (1)$$

$$cos\theta_D = f_1 cos\theta_{eq} - f_2 \quad (2)$$

where r, f_1 and f_2 are the surface roughness, the total area of the solid–liquid interface and the total area of liquid–gas interface in a plane geometrical area, respectively. Accordingly, the free energy of a droplet in the Cassie–Baxter state is smaller than that of the Wenzel state, so it is well expected that the droplet should be in the Cassie–Baxter state when being driven.

2.2. Liquid Marbles from Nature to Lab

An LM is a nonwetting droplet system, generally consisting of a liquid core and a particle shell, Figure 3a. Its prototype is also derived from the natural world. In order to avoid the problem caused by the honeydew that accumulates in the habitat, the aphid secretes wax particles to wrap the honeydew, which can be easily pushed and removed, Figure 3b [44]. This product, prepared by the aphids for survival, was gradually discovered by scholars and named as LMs [45]. Interestingly, after extensive research, it was found that the protection of the particle shell allows LMs to operate not only on solid surfaces but also on liquid surfaces and even inside another liquid [25,26]. Furthermore, LMs show many advantages over bare droplets, including good robustness, slow evaporation, high elasticity and low friction. Considering these advantages, LMs have been developed as advanced micro-reactors or sensors that could be widely used in cell culture, diagnostics and therapeutics [23,46–50]. The widespread application of LMs relies heavily on their overall quality, which is largely dependent on the combination choice of core liquid and coating particles. The viscosity and volume of the core liquid, as well as the size and the hydrophobicity of the coating particles all contribute to the properties and performance of LMs to a certain extent. This section thus focuses on the formation mechanism of LMs and outlines the particulate factors that affect their whole performance.

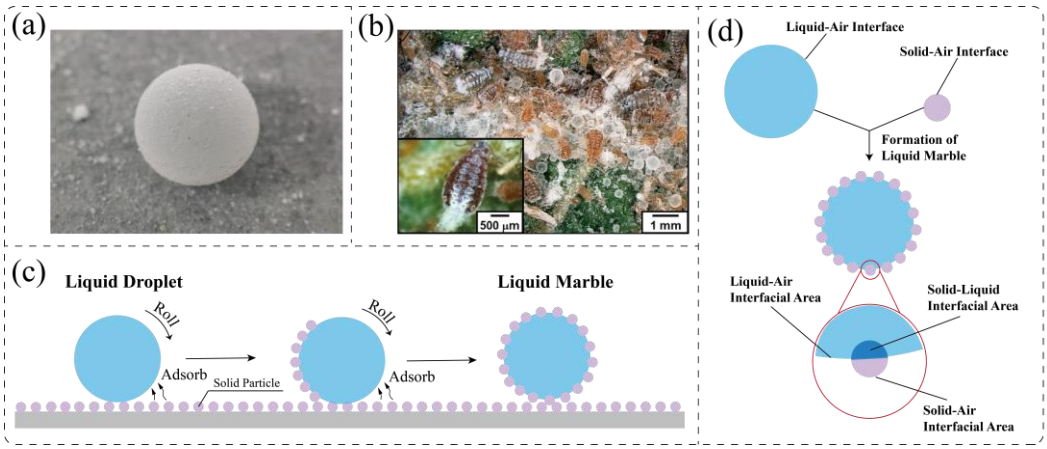

Figure 3. (**a**) An artificial LM from the lab. (**b**) Natural LMs fabricated by aphids [44] (Reproduced with permission from American Chemical Society, 2019). (**c**) Schematic of the formation process of an LM. (**d**) Schematic of interface changes during LM formation.

2.2.1. Formation Mechanism

The formation of an LM involves a simple process whereby hydrophobic particles spontaneously arm onto the surface of a liquid droplet, Figure 3c. The principle of surface energy minimization could be adopted to explain the particle arming process. In this process, it is assumed that the coating particles are smooth and uniform and the random deposition of particles onto the droplet does not change the original liquid surface area. Comparing the surface free energy G of the core–shell system before and after LM formation, only two parts of G will be changed here: a part of the solid–air interfacial area A_{SA} converts to the solid–liquid interfacial area A_{SL}, while a part of the liquid–air interfacial area A_{LA} of the droplet is occupied by particle aggregates, Figure 3d. Calculating the corresponding surface free energy G of interface changed regions as:

Before particle adsorption

$$G_1 = \gamma_{SA} A_{SA} + \gamma_{LA} A_{LA} \tag{3}$$

After particle adsorption

$$G_2 = \gamma_{SL} A_{SL} \tag{4}$$

where γ_{SA}, γ_{LA} and γ_{SL} are the interfacial tension of the solid–air, liquid–air and solid–liquid interface, respectively. Therefore, the energy difference ΔG among them can be deduced as:

$$\Delta G = (\gamma_{SL} - \gamma_{SA}) A_{SA} - \gamma_{LA} A_{LA} \tag{5}$$

According to Young's law, the energy difference ΔG of LM formation further turns to [51]:

$$\Delta G = -\left(cos\theta_{eq} A_{SA} + A_{LA}\right) \gamma_{LA} \tag{6}$$

And the ratio of liquid–air interfacial area to solid–air interfacial area is expressed as:

$$\frac{A_{LA}}{A_{SA}} = \frac{1 - cos\theta_{eq}}{2} \tag{7}$$

In a simplified model, the ratio could be either zero or greater than zero [51]. As a result, ΔG must be less than zero, which means the surface free energy of the system consisting of the liquid droplet and solid particles becomes less than that of a single droplet. Thus, the arming process is instinctively spontaneous and the final core–shell system should be stable without extra interventions.

2.2.2. Particle Effects on Marble Performance

The stability of LMs represents their capability to withstand external disturbances. Higher stability means that LMs can bear more vital external forces, which is an essential prerequisite for LMs to work in various environments. The lifetime of LMs determines its survival time. In other words, the longer lifetime, the longer the service time, which is critical to the biological applications of LMs. Unlike bare droplets on a solid surface, whose performance is only directed by liquid properties and environmental factors, the robustness and lifetime of LMs can also be greatly affected by particle properties, such as hydrophobicity, size and the number of layers, Figure 4 [52].

While preparing LMs, both hydrophilic and hydrophobic particles could be used. However, particles with various wettabilities bring about different properties. In order to obtain a more stable LM, particles with a contact angle $\theta = 90^{\circ}$ are preferred for maintaining the smallest surface energy in theory [51,53,54]. To obtain a longer service period, coating particles with higher hydrophobicity are in needed [55]. The size of coating particles becomes another vital factor to be considered. In the monolayer state, LMs prepared by larger-sized particles tend to be more stable. This conclusion has been drawn in stability experiments of LMs [56,57]. Nevertheless, an increase in the particle size leads to a decrease in the effective surface tension and consequently reduces the lifetime of floating LMs on the

water surface [55]. In addition, the size of coating particles constantly affects the layout of particles on the droplet surface, with larger particles forming monolayers and smaller ones forming multilayers [58,59]. Also, the number of particle layers is key to determining the overall performance of LMs [60]. Generally, multilayered LMs have better mechanical robustness than those monolayered marbles [59,61,62]. At the same time, multilayered LMs have a longer lifetime than monolayered LMs. It is because the single-layer LMs expose more liquid–air interface than bare droplets owing to the incompressibility of the interface, dry much faster instead. However, for multilayered LMs, due to the rapid rise of the ratio between the height of the porous media and the typical length of the interface, the drying rate will slow down obviously [63].

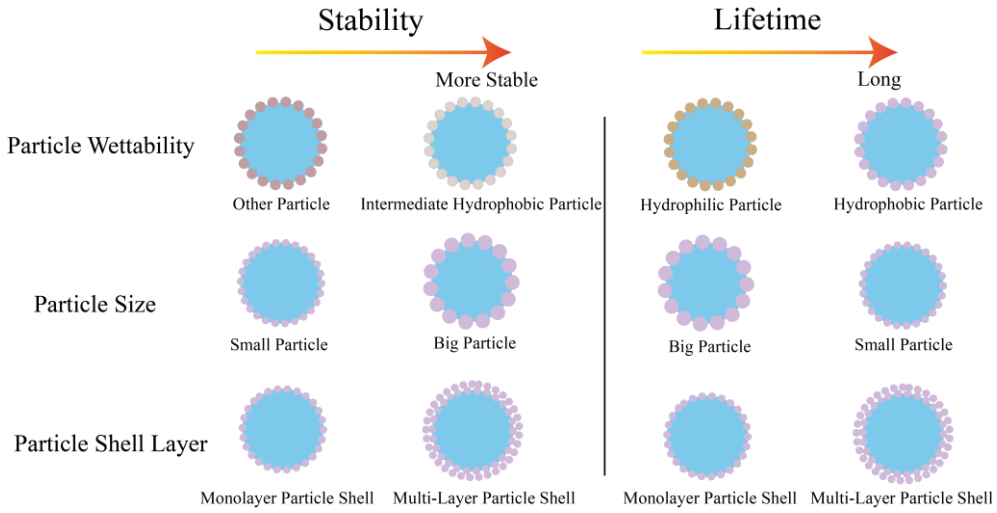

Figure 4. The stability and lifetime of various LMs with different types of particle shells.

2.3. Friction Obstacles in Driving Small-Volume Liquid

Friction is common in life and often acts as a hindrance most of the time, increasing unavoidable energy consumption. The process of driving droplets on solids cannot either avoid the obstruction of friction. However, the friction mechanism of droplets on a solid surface is quite different from that of the solid–solid friction, as its friction force is attributed to the viscosity of the fluid. The friction mechanism of droplets on a solid surface can be divided into static and dynamic forms, where static friction is always greater than dynamic friction [64]. Interestingly, the nonstick property of the droplet on a superhydrophobic surface makes it possible to roll like a sphere, resulting in the corresponding friction mechanism being further altered, Figure 5a [65–67]. By contrast, LMs generally exhibit a similar or even better nonstick property than bare droplets on a superhydrophobic surface. The reason behind this is that bare droplets contact with the substrate directly, while LMs are separated from the substrate by a large number of air cushions and solid particles, Figure 5b. Hence, there should exist some differences in the friction mechanism between LMs and droplets. Nevertheless, when studying the motion of LMs, they are still treated as spherical droplets on a continuous superhydrophobic surface, which is clearly different from their discrete particle distribution. In addition, it is worth noting that there is a special case of the LM–substrate contact. When the particle shell of an LM is monolayered and the particles are quite small (~nm), the intermolecular force can be prominent and the liquid core will come into direct contact with the substrate below [61]. This contact form differs from those of conventional LMs and also of bare droplets. Therefore, this unique LM may have unique dynamic behaviors in movement.

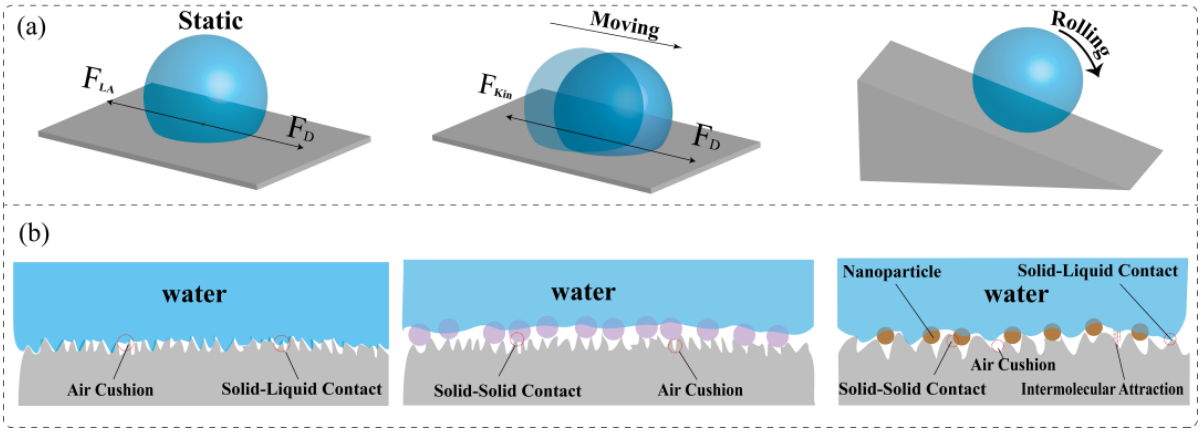

Figure 5. (**a**) Schematic of three different kinematic states of droplets on a solid surface. (**b**) Snapshots of contacting areas for a droplet, a conventional LM, and a monolayer nanoparticle-covered LM on solid substrates, respectively.

The friction of droplets on a solid surface is manifested as lateral adhesion force, and when acting together with external forces the droplets will be deformed, forming a contact angle difference in the front and rear directions (θ_{Rear} and θ_{Front}). Subsequently, when the external force is large enough, the contact angle difference will exceed the tolerance range and the induced movement happens [64]. Thus, the static lateral adhesion force F_{LA} can be described by the surface tension, the contact angles and the contact width L of the droplet [68]:

$$F_{LA} = kL\gamma_{LA}(cos\theta_{Rear} - cos\theta_{Front}) \tag{8}$$

The dimensionless factor k here accounts for the precise shape of the solid/liquid/air three-phase contact line of the droplet, which was calculated to be between $1/2$ and $\pi/2$. Therefore, to drive a bare droplet on a solid surface, the drive force F_D needs to be strong enough to defeat the static lateral adhesion force F_{LA}. When the motion starts, the static lateral adhesion force F_{LA} converts to the kinetic viscous force F_{Kin}. For keeping the motion of the bare droplet, F_D must balance F_{Kin} carefully after the motion is initiated [64].

The friction mechanism of a droplet rolling on a superhydrophobic surface is related to the viscosity of the liquid, and its steady velocity on an inclined surface is determined by the rate of energy dissipation versus the rate of change of gravitational potential energy [65]. Similarly, the friction mechanism of an LM is also attributed to the viscosity of the liquid core and can be subdivided into two types. One is the energy consumption to break the contact line, and the other is the viscous dissipation in the bulk of LMs [69,70].

Based on the motion of nonwetting droplets, it is known that bulk viscous dissipation is an important factor in the deceleration of these droplets, and its energy dissipation rate $\dot{E}$ can be estimated by the following equation [69]:

$$\dot{E} = \eta \int_{V_d} \left(\vec{u}\right)^2 d\Omega \tag{9}$$

where η is the viscosity of the liquid, V_d is the volume over which viscous dissipation occurs and $\vec{u}$ is the velocity field in the droplet and $d\Omega$ is the micro-element volume. According to the energy conservation law, the deceleration of a nonwetting droplet can be described as:

$$\dot{E}\tau = \frac{7}{10} m u_0^2 \tag{10}$$

where $\tau \cong 2S/u_0$ is the time of slowing, m is the mass of the droplet and u_0 is the initial velocity of the marble center of mass. Considering the $\left|\nabla \vec{u}\right| \cong u_0/R_0$, in which R_0 is the

radius of the droplet, $V_d \approx l^3$, l is the radius of the contact area and $m = \frac{4}{3}\rho\pi R_0^3$, so the distance necessary for stopping S can be calculated by [65]:

$$S = 1.5\frac{\rho u_0 R_0^2}{\eta l^2} \tag{11}$$

This is the formula for the motion distance of LMs under the control of body viscous dissipation. With this equation, the friction mechanism of LMs can be initially judged and then the driving strategy can be adjusted based on the detailed friction mechanism [69].

A further difference to bare droplets is that LMs can stably float on a liquid surface. An LM floating on a liquid surface will often form a meniscus, which makes the friction mechanism differ from those of the LMs on a solid surface and also in the carrier liquid. This interesting feature enables more choices of transportation for LMs [27]. For calculating the Stokes drag F_f force in transportation, the effect of the meniscus must be taken into account, and a correction factor has to be introduced [71,72]:

$$F_f = 6\pi\beta\mu R_0 v \tag{12}$$

where μ is the dynamic viscosity of the carrier liquid, v is the horizontal velocity of the LM, and β is the correction factor for the coefficient of friction. The friction is not a fixed value but is proportional to the velocity, which is consistent with the motion of an object in a liquid.

2.4. Actuation Principles of Small-Volume Liquid

As mentioned above, the primary obstruction to the smooth motion of droplets comes from lateral adhesion force. Meanwhile, an LM confronts less resistance because of the presence of a particle shell and thus its motion on the liquid surface presents a different frictional mechanism. Regardless of the detailed friction mechanism, the motion will be initiated anyway, as long as the applied driving force is strong enough. With the advancement of theory research and manipulation technology, more actuation strategies have emerged for overcoming friction in transporting small-volume liquid. The principles of these strategies can be mainly classified into wettability gradients, body forces and other schemes for special purposes, Figure 6.

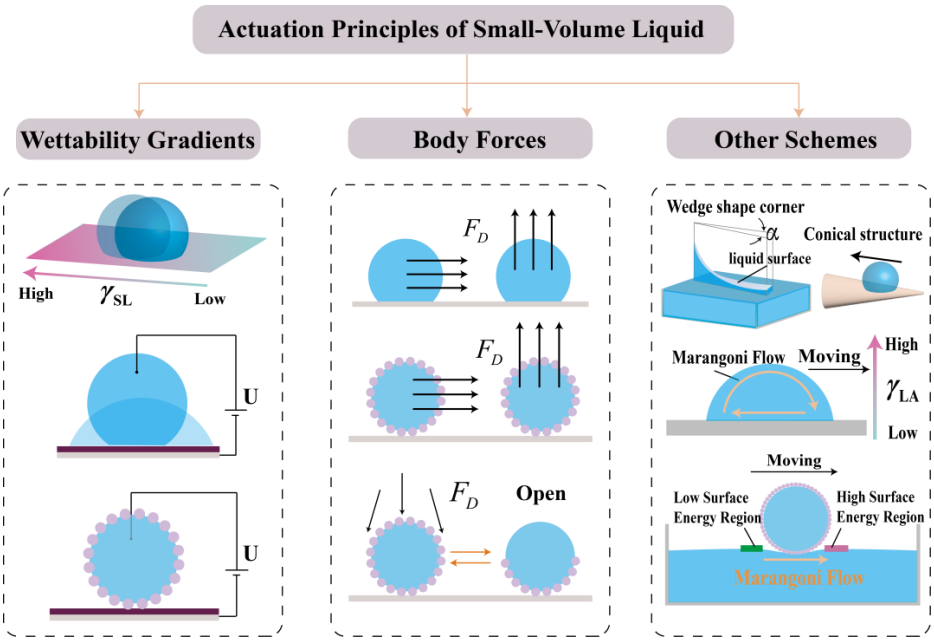

Figure 6. The actuation principles of small-volume liquid, with subcategories of wettability gradients, body forces and other schemes.

2.4.1. Wettability Gradients

Solid surfaces are generally considered to be isotropic and their surface energy should be uniform in all directions. The total energy U_γ of a droplet on these solid surfaces is thus identified as a constant. However, when there is a surface energy gradient on the solid surface, the total energy of the droplet–surface system will have a spatial gradient, which eventually creates a driving force to move the droplet. A general expression for the driving force is given as [31]:

$$F_D = -\nabla U_\gamma \tag{13}$$

Wettability is the macroscopic manifestation of the difference in the surface energy of a solid surface. Hence, the driving force can be expressed with the contact angle as follows:

$$F_D = \pi l^2 \gamma_{LV} \frac{dcos\theta}{dx} \tag{14}$$

Here θ is the contact angle of the droplet to the surface, which is a function of the position x of the plane. The detailed expression of the driving force depends on how the wettability gradient is generated. When the wettability gradient is created by surface chemistry, the contact angle of the droplet is determined by the chemical composition of each location, and the driving force can be expressed by Equation (14) [73]. Moreover, to modulate droplet motion more easily, the substrate surface can be modified with stimuli-responsive molecules that change wettability in response to external stimuli. When the wettability gradient is formed by adjusting roughness instead, the contact angle needs to be modified according to the characteristics of the surface microstructure, so that the driving force expression will be adapted [74]:

$$F_D = \pi l^2 \gamma_{LV} \frac{d\phi}{dx} (cos\theta_{eq} + 1) \tag{15}$$

where ϕ is the surface area fraction. The actuation methods that focus on the substrate surface, although they are effective in driving bare droplets, do not work for an LM. This is because the over-protection of the particle shell causes the liquid core of the LM to be isolated from the substrate, preventing it from responding to the change in substrates.

Electrowetting is also a useful phenomenon that can be adopted to actuate droplets. This phenomenon shows highly controllable characteristics after introducing a dielectric layer (known as electrowetting on dielectric, EWOD) and has been widely used in droplet manipulation [75]. Its actuation principle can also be attributed to the wettability gradients. The surface tension of a droplet on a dielectric layer becomes smaller under the influence of the voltage, and the Lippmann equation can describe its variation [76]:

$$\gamma_{SL}(V) = \gamma_{SL} - \frac{\varepsilon_0 \varepsilon_r}{2d} V^2 \tag{16}$$

where V is the voltage, ε_0 is the vacuum dielectric constant, ε_r and d are the effective dielectric constant and the thickness of the dielectric layer, respectively. The decrease in solid–liquid surface tension will eventually lead to a decrease in the contact angle of the droplet, which can be obtained by combining Young's equation and Equation (16) [75]:

$$cos\theta_{eq}^{U} = cos\theta_{eq} - \frac{\varepsilon_0 \varepsilon_r}{2d\gamma_{LV}} V^2 \tag{17}$$

Combining the equation above with Equation (14) will yield the driving force of this electrowetting actuation method. Unlike previous methods of modifying substrates, electrowetting directly affects the liquid content. Therefore, the electrowetting approach can not only achieve the driving of bare droplets efficiently but also apply to the effective actuation of various LMs [77].

2.4.2. Body Forces

The body force means a noncontact force that can act uniformly on each volume element of the target body. Hence, body forces are a good choice in manipulating all types of liquid with small volumes. The most common body force is gravity, which often spears in the actuation of droplets and LMs. Examples of gravity-driven droplets are easy to find in life, such as the fall of a raindrop, or the sliding of a droplet on a car's windshield. Unfortunately, gravitational droplet actuation exhibits many inherent restrictions. For instance, it cannot be manually controlled and is always downwards. As a consequence, the motion direction of both droplets and LMs is fixed. Apart from gravity, some other body forces can also be used to drive small volumes of liquid. These body forces, including but not limited to electric, magnetic, and sound fields induced forces, possess distinctive features that are attractive in manipulation and beyond.

When a small-volume liquid carries free electrons, the free electrons will be redistributed on the surface by the presence of an electric field and eventually generate an electrostatic force [78]. In contrast, an electric dipole can be formed for liquids without electrons in the electric field, due to the electric polarization. When the electric field is nonhomogeneous, the forces at the different ends of the liquid volume are not equal, and may even move small-volume liquid against gravity [79]. This dielectrophoretic force can be calculated by the following equation [80]:

$$F_D = 2\pi R^3 \varepsilon_1 \left[\frac{(\varepsilon_2 - \varepsilon_1)}{(\varepsilon_2 + 2\varepsilon_1)} \right] \nabla U^2 \tag{18}$$

where R is the radius of the small-volume liquid, U is the electric field, ε_1 and ε_2 are the dielectric constants of the liquid and the environment, respectively. By contrast, when the external field is a magnetic field, it is generally necessary to add magnetic components to the droplet-based system. Otherwise, it cannot effectively responds to the magnetic field applied. The corresponding driving force F_m comes from the magnetic field and can be calculated by the following equation [81]:

$$F_m = \left(\frac{M}{\rho} \right) \chi \frac{B_m}{\mu_0} \nabla B_m \tag{19}$$

where M is the mass of the magnet, χ is the magnetic susceptibility of the magnetic particles, B_m is the magnetic field applied, and μ_0 is the permittivity of free space. However, the main concern is that the magnetic particles may detach when the resistance is greater than the capillary force for adsorbing particles in bare droplets and especially LMs.

In terms of the acoustic field, the propagation of sound energy is simpler and more direct. Acoustic waves can inspire any object within the field theoretically, and the movement of small-volume liquid can be easily achieved through fine control of waveforms [82–85]. Unfortunately, due to the complicated action form of acoustic waves, the driving force of the acoustic field is hard to be derived quantitatively in the same way as calculating either electric or magnetic force. Despite this, this body force still attracts scholars' interest [86]. Part of the reason is that its contactless nature shows a significant advantage, making it not easy to fail in LM manipulation, just as the wettability gradient does. In addition, this avoids the cross-contamination of target droplets and LMs from contacting with external objects. In summary, apart from being able to drive droplets and LMs simply, the body force enables a controlled operation that is also meaningful for LMs, namely the reversible opening and closing of the particle shell, which will be discussed in detail in the following section.

2.4.3. Other Schemes

Surface tension affects the wettability of droplets and is also responsible for the rise of liquid in capillary tubes. When a wettable capillary tube is inserted into a liquid, the liquid will climb up against gravity under the influence of surface tension. Additionally, the formation of Laplace pressure difference is also related to surface tension. When the

liquid surface is in a curved state, a Laplace pressure difference appears between the inside and outside of the curved liquid surface under the action of surface tension. With some special structures, the capillary rise and Laplace phenomena can be employed together for the transfer of small volumes of liquid [87]. Furthermore, the Marangoni flow is also a valid method to drive tiny droplets, aided by the surface tension difference induced by a temperature or concentration gradient [73,88]. Apart from being able to drive droplets on solid surfaces, Marangoni flow can also drive LMs on liquid surfaces in a unique way [89]. Using similar temperature or concentration gradients, a surface tension difference will be induced near the carrier fluid of floating LMs and thus Marangoni flow generates. Eventually, independent LMs tend to move with the flow of the carrier fluid [25,90]. This interesting carrier-based driving method efficiently actuates LMs on various liquid surfaces, enabling floating LMs to function as a versatile platform with tremendous potential.

The transportation of droplets can be efficiently achieved by machining the wedge-shaped corner structure. In this structure, the liquid will rise, which is consistent with the phenomenon of capillary rise in life and the rise in height H can be determined by the equation below [91]:

$$H = \frac{2\gamma_{LV} cos\theta_{eq}}{\rho \alpha g y} \tag{20}$$

where α is the wedge angle and y is the position of the liquid surface. If there is a wedge angle gradient from bottom to top, the rise height will be larger. In addition, the conical structure with a radial gradient is valid for droplets' spontaneous motion. According to the Laplace equation, the value of the pressure difference is inversely proportional to the radius of curvature. The total Laplace pressure is zero when the substrate surface is flat, and the Laplace pressure becomes asymmetric when the substrate surface has a structural gradient, which can be used to transport droplets. The driving force of a droplet on the conical structure can be calculated by the following two equations [92]:

$$F_{Laplace-hydrophilic} = \gamma_{LV}\left(\frac{1}{R_1} - \frac{1}{R_2}\right) S_{TCL-barrel} \tag{21}$$

$$F_{Laplace-hydrophobic} = \gamma_{LV}\left(\frac{1}{R_1} - \frac{1}{R_2}\right) S_{TCL-clamshell} \tag{22}$$

where $S_{TCL-barrel}$ and $S_{TCL-clamshell}$ represent two forms of three-phase contact lines for droplets on a conical structure, R_1 and R_2 are respectively the local radii of the conical structure at two opposite sides of the droplets. Not surprisingly, these two transportation methods for small-volume liquid based on special structures also severely rely on the perception of the substrate surface. As a result, LMs cannot be aided by these two special structures to release their fantastic performance.

3. Transportation of Bare Droplets and Liquid Marbles

The versatile application of small-volume liquid heavily relies on the detailed means of manipulation, particularly the way of transportation, one of the most fundamental tasks in liquid manipulation. However, different transportation methods have respective requirements or technical restrictions on the wide use of droplets and LMs, which are serving as independent systems in OMF. For instance, traditional transportation based on different substrate surfaces requires small volumes of liquid to contact well with the surface and delicate surface processing is needed. Transportation assisted by external fields often requires a precise adjustment of the action of these fields. In more detail, the droplet motion on the solid surface with a wettability gradient usually involves processing microstructures or regulating surface chemistry [93–95]. Particularly, the motion on some special surfaces demands the machining of specific morphological features, such as the wedge corner and the conical structure [35,96]. In addition, the use of Marangoni flow to drive droplets and LMs requires fine control of the liquid components. Furthermore, for external fields, the transportation driven by an electric field must be controlled under an appropriate voltage;

otherwise, irreversible damage to the system will occur [97,98]. The magnetic-field actuated transportation needs the incorporation of magnetic materials anyway and these materials tend to detach in moving under a strong magnetic field [99–101]. Moreover, the propagation of acoustic or light fields is affected by the relevant working environment, so acoustic- and optical-driven motions may only be adopted on specific occasions [26,84,102,103]. Based on the detailed mechanisms, the transportation of droplets and LMs here can be systematically classified as spontaneous motions and motions with external assistance, as illustrated by Table 1.

Table 1. The approaches, driving force, and principles in both the spontaneous motions and external-field actuated motions of bare droplets and LMs (note: Different quantities of "○"and "◎" symbolize the relative capacity of various approaches in actuating bare droplets and LMs, respectively).

Motion Forms	Approaches		Driving Force	Principles
Spontaneous motions	surface textures surface chemistry	○○ ○○	surface tension	surface texture gradient surface chemistry gradient
	Marangoni flow	○/◎	surface tension	temperature gradient concentration gradient
	wedge corner conical structure	○ ○	capillary force Laplace pressure	gradient structures
Motions with external assistance	electric field	○○○/◎◎◎	electrostatic force dielectrophoretic force surface tension	electrostatic effect dielectrophoresis electrowetting
	magnetic field	○○/◎◎◎	magnetic force	magnetic field action
	acoustic field	○○/◎◎	acoustic force	acoustic wave action
	optical field	○/◎◎	surface tension	optical-induced temperature gradient optical-induced molecular structure change

3.1. Spontaneous Motions

As a common form in liquid transportation, spontaneous motions can be easily achieved by changing environmental factors, where a tiny liquid can move smoothly without the assistance of an external field. Modifying or manufacturing the substrate surface with different wettabilities and morphologies is usually an efficient way to realize spontaneous droplet motion. Recently, many types of specific substrates have been artificially fabricated and applied in droplet transportation, such as the substrate with a wettability gradient, a wedge-shaped corner structure, and a conical structure. This approach lies in the fine modification of solid substrates, so it cannot be used for inducing the spontaneous motion of LMs. However, the actuation using the Marangoni flow is a type of carrier-based transportation that does not ask for liquid contents to sense substrate structures. Its unique actuation principle permits an LM to have spontaneous motions as well, but the motion is so arbitrary that it is hard to predict its routes. Generally, the advantages of spontaneous motions for small-volume liquid are obvious. Once the change of environmental factors is accomplished, the small volume of liquid will follow a predetermined route to move and no extra energy will be consumed during the entire process. Moreover, proper modifications to multiple substrate properties can be combined to greatly enhance the efficiency of transportation. Nevertheless, the spontaneous motion of droplets and LMs also exhibits some drawbacks, for example, the single path and the inability to regulate readily.

3.1.1. Surface Textures

In 1978, Greenspan first pointed out that a water droplet would spontaneously move when the substrate had a wettability gradient [104]. Whereafter, the motion mechanism of droplets moving on a solid substrate was analyzed [105]. With this concept proven, more researchers have developed numerous methods to process wettability gradients and then achieved various spontaneous motions of small-volume liquid [93,96,106]. Among these methods, manufacturing surfaces with different degrees of roughness for controlling the wettability gradient is one of the most classical methods. Advances in micro- and nano-fabrication technologies offer a variety of options for processing surface texture gradients, including scanning probe lithography, photolithography and scanning beam

lithography. Readers can learn more details in a review that summaries the novel technologies on microstructure and nanostructure fabrication [106]. Furthermore, this review also offers a decision-making tool for helping researchers identify which strategy to choose for fabricating the structure with predefined properties. A recent study has demonstrated the concept of scalable multifunctional surfaces and structural gradients on graphene-related materials [93], showing variations in the structure, wettability and other properties. This study presents another viable approach to processing surface textures. In another work inspired by the natural mist collection of nano-buccal beetles and desert cacti [96], porous copper nanopillars were manually prepared on a curved surface of acupuncture needles with glancing angle deposition. This work successfully combines the Laplace pressure difference induced by the curved structure and the wettability gradient, improving the efficiency of mist droplet collection greatly, Figure 7a.

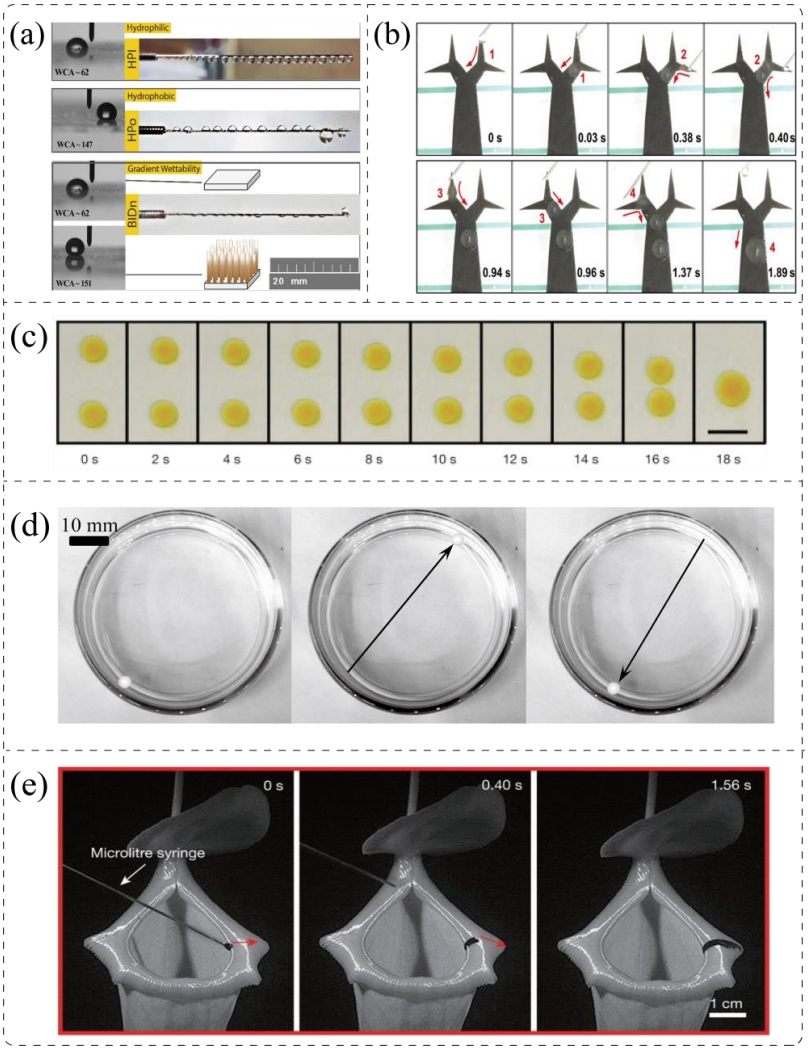

Figure 7. (**a**) Fog collection with a hydrophilic needle, a superhydrophobic needle and a bioinspired design needle respectively from top to down [96] (Reproduced with permission from American Chemical Society, 2021). (**b**) Aggregation and motion of droplets on horizontally positioned multiple-shape gradient surfaces [107] (Reproduced with permission from American Chemical Society, 2017). (**c**) Two droplets attract each other and coalesce due to the Marangoni flow (scale bar: 5 mm) [89] (Reproduced with permission from Springer Nature, 2015). (**d**) The motion of an LM containing 70 vol% aqueous ethanol solution, which is caused by the Marangoni flow of the water carrier [90] (Reproduced with permission from American Chemical Society, 2015). (**e**) Anti-gravitational droplet motion on the structure of wedge corner with an opening angle gradient [35] (Reproduced with permission from Springer Nature, 2016).

3.1.2. Surface Chemistry

Another classical method of creating a wettability gradient is to control surface chemistry. The surface chemistry gradient is usually determined by surface functional groups. Thus, adjusting the functional group composition or concentration of the substrate can effectively regulate the related surface energy. In 1992, Whitesides et al. first utilized chemical gradients to achieve a spontaneous motion of droplets, by depositing silanes on a carrier surface [105]. Subsequently, a variety of creative strategies have been developed to fabricate chemical gradient surfaces for realizing spontaneous droplet motion. For example, a way to transform self-assembled films on silicon and gold substrates into gradient surfaces was reported by Han's team, named the "space-limited plasma oxidation" method [108]. Hernández's group developed another simple strategy to produce a chemical gradient on the graphene surface, which just used a physical mask to cover the surface during plasma processing [94].

The driving capability of the wedge-shaped pattern surface with a width gradient comes from the difference in wettability between two sides of the contact line. By setting the wedge-shaped part of the pattern as hydrophilic and the other part as hydrophobic, transportation occurred when droplets touched the contact line of these two parts, Figure 7b [95,107]. For example, Li and his team prepared a sample of a wedge-shaped surface with Ag/Cu by adhering to a wedge-shaped mask on copper and then dipping the whole into $Ag(NH_3)_2OH$ for the reaction [95]. Subsequently, they placed a droplet with 30 vol % PG on this wedge-shaped surface. The shape of the droplet became irregular in the limit of the wedge-shaped contact line. Eventually, due to the asymmetry of the shape, a water vapor difference appeared in the vicinity of the droplet and the Marangoni stresses that could drive the droplet were then generated.

3.1.3. Marangoni Flow

Marangoni flow is mainly attributed to surface tension gradients and occurs where the difference of surface tension exists at the liquid interface. Cira et al. mixed propylene glycol with water to produce two-component droplets that showed significant volatility and surface tension differences. When these droplets were deposited at distances of several radii, the water vapor at the adjacent end would interact. This interaction resulted in less evaporation of water at the adjacent end than that at the distal end, which further caused a difference in the concentration of propylene glycol. Hence an asymmetry in surface tension would occur at both ends, resulting in a reasonable driving force [89]. Finally, this force would defeat the viscous drag force and achieve droplet motion and coalescence, Figure 7c. A similar approach can also be used for LMs' transportation. Bormashenko and co-workers placed LMs prepared from the mixture of alcohol and water on a water surface [90]. The alcohol in the LM evaporated from the micropores among coating particles and condensation occurred when the alcohol vapor reached the water surface, leading to a local decrease in surface tension on the water surface. Once the alcohol in the LMs evaporated asymmetrically, a surface tension gradient appeared around the LMs on the water surface and then Marangoni flow would emerge to drive the LMs randomly, Figure 7d.

3.1.4. Substrate Structures

Apart from the wettability gradient and the Marangoni flow, some other meaningful schemes can also realize the spontaneous motion of droplets. Generally, the scheme of processing special structures on substrates differs from those schemes with wettability gradients, and its driving force usually comes from the capillary force or Laplace force. There are two types of special structures in driving droplets: the structure of the wedge corner and the conical structure with a radius gradient. Interestingly, processing an opening angle gradient on the structure of the wedge corner can effectively increase the height of anti-gravitational rise with the help of capillary force, Figure 7e [35]. For the conical structure with a radius gradient, it is often found on plants in nature for collecting water

mist, whose driving force comes from the Laplace pressure difference caused by a radius gradient. However, the gradient of Laplace pressure difference has a limited ability to drive droplets, so it is usually combined with a wettability gradient to improve the driving efficiency. More details on the droplet motion by utilizing structure gradients could be found in a recent review by Li and Guo [87].

3.2. Motions with External Assistance

There are two categories in which the external field can achieve the motion of a small-volume liquid. The first one is attributed to an indirect effect. This category achieves motions indirectly by modulating the properties of droplets and LMs or even the surrounding environment, such as temperature, surface wettability, and substrate morphology. The success of these indirect motions owes to the emergence of responsive materials, mainly magnetically and optically responsive materials. The application of these materials enhances the motion controllability of droplet-based systems, allowing the motion to be flexibly adjusted in time and spatial dimensions. The well-known EWOD method can be classified into this category. Another category is applying an external force directly to the small-volume liquid system to overcome the friction resistance and realize controllable actuation. These direct forces mainly come from electric, magnetic and acoustic fields. This category has an obvious advantage of transient responsiveness, which enables the direction of external forces to switch in seconds. However, these forces applied directly on liquid targets, especially LMs, have to be finely controlled to avoid system destruction. For example, strong electric or acoustic fields may cause unpredictable damage to the particle shell of LMs, and uncertain magnetic fields would make the magnetic materials around LMs detach anytime.

3.2.1. Electric Field

As one of the most common energy sources, the electric field plays an important role in microfluidics, especially droplet microfluidics. Numerous studies have demonstrated that the electric field can easily transport small-volume liquid on various substrates, and even some usual electrical phenomena in our daily life, such as electrostatic induction, can be adopted to transport droplets. Washizu et al. have implemented electrostatic driving through a delicate electrode arrangement [109]. They placed a droplet on a hydrophobic insulating layer-coated substrate with electrodes on the bottom. Once the electrode near the droplet was energized, the droplet generated induced charges and then moved toward the electrode under the electrostatic force, Figure 8a. The use of electrostatic force is also an effective way to transport LMs. When a charged cylinder approached an LM, similar movements were observed [70]. Bormashenko's group investigated the transportation of LMs in an electric field [110], confirming the use of the electric field to promote the climbing of liquid parts inside a composite LM composed of diiodomethane (or methylene iodide) and water, Figure 8b. This unique marble transportation behavior can be attributed to the dielectric force from molecular polarization, which requires neither the modification of the particle nor the liquid core, and thus it has since been widely used in the manipulation of LMs. In terms of adopting dielectrophoretic force to transport LMs, the study reported by Ooi and co-workers is worthy of attention [111]. The team has successfully achieved the picking up and placing of LMs at specified positions by using an electrode with a high-voltage bias, Figure 8c. When the lifting force derived from the effect of dielectrophoresis was stronger than gravity, the LM was picked up and then could be transferred vertically. Moreover, they investigated the effect of a nonuniform direct current (DC) electric field on actuating floating LMs [71]. Subsequently, Jin et al. have further expanded and enriched the application of dielectrophoretic force in manipulating various LMs and realized the trapping and positioning of a floating LM by specific electrode configurations, Figure 8d [112,113].

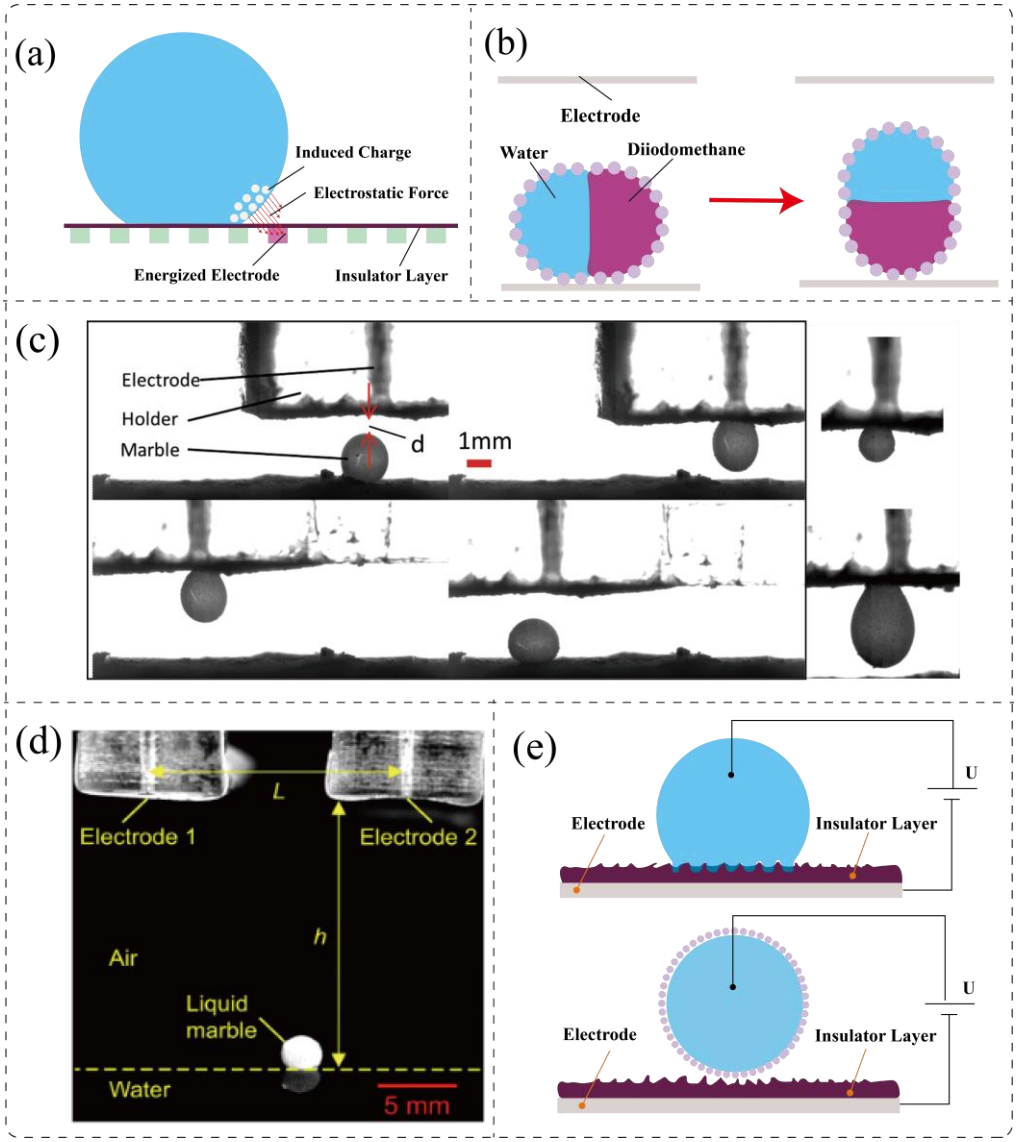

Figure 8. (**a**) A droplet moving on a hydrophobic insulating substrate under the electrostatic force caused by specific energized electrodes. (**b**) Schematic of a water marble climbing on the methylene iodide marble in an electric field [110]. (**c**) Snapshots of a picking-up and placing process of LMs through dielectrophoretic force [111] (Reproduced with permission from Springer Nature, 2018). (**d**) The positioning of a floating LM by the dielectrophoretic force [113] (Reproduced with permission from Springer Nature, 2019). (**e**) The comparison of a droplet and an LM actuated by EWOD, respectively.

Among various ways to accomplish small-volume liquid transportation using electric fields, the electrowetting phenomenon is worthy to be considered. As an indirect way to drive droplets, the direct driving force of electrowetting comes from the modulation of surface tension by the electric field [76]. To avoid droplet electrolysis caused by the effect of working electrodes, a dielectric layer is needed and usually coated uniformly on the electrode, namely EWOD. In early studies [114], most designs of EWOD were grounded by clamping a grounding plate to the droplet or inserting a wire into the droplet, showing certain limitations in driving droplets. Later, the design of the EWOD was gradually improved and it is possible to ground from the dielectric layer, greatly increasing the flexibility of droplet transportation [115]. The EWOD way is also a boon for driving LMs. This way avoids the requirement to touch the substrate and directly affects the liquid inside LMs. Moreover, the combination of EWOD with separate LMs solves the dilemma of droplets in electrowetting actuation. The electrocapillary pressure may cause the droplet

to be irreversibly trapped in the gaps of microstructures on a superhydrophobic surface, while an LM cannot penetrate the microscopic voids of the substrate with its core liquid due to the presence of the particle shell, Figure 8e [98]. Nevertheless, constant attention needs to be paid to the state of LMs when the voltage is increased, because the liquid can penetrate the coating particles at excessive working voltages and some particles may even be ejected from the marble surface randomly [77]. Despite all this, the transportation of small-volume liquid employing electrowetting is still an effective and promising approach.

3.2.2. Magnetic Field

Magnetic actuation is a quite convenient means to implement oriented transportation, even with a small permanent magnet. Therefore, actuation strategies based on magnetic fields are attracting more interest from researchers. For efficient transportation, the most straightforward approach is to add enough magnetic particles into the droplet and then utilize the magnetic force to overcome motion frictions. However, the detachment of magnetic particles is a critical issue that has to be considered, as mentioned in the study of the fundamentals of magnetically driven droplets by Long's team [81]. To demonstrate the feasibility of magnetic manipulation, Zhang et al. combined the droplets containing magnetic particles with substrates carrying surface energy traps, completing the all-round operations of droplets, Figure 9a [116]. Yang's group used a superhydrophobic electromagnet needle to attract the magnetic beads inside a droplet, which lifted the droplet and allowed the droplet to move freely [117]. Later, Li and co-workers further simplified the approach to operate droplets with magnetic particles [100]. This team used only two steel beads and a magnetic control system to realize the transportation, splitting, releasing and rotation of different droplets. A few interesting methods that even do not require magnetic particles tightly bound with droplets have also been reported. Recently, some researchers have used magnetically responsive materials as substrates. The surface topography of these substrates could be governed by magnetic fields, which have been demonstrated in actuating droplets indirectly [118,119]. Furthermore, Fan et al. reported a more exciting way to actuate droplets that could change the droplet into a crescent shape and even realize cargo transfer [120]. This is because the properties of a ferrofluid droplet allow it to satisfy a variety of shape requirements under the control of a magnetic field. This team precisely regulated the shape of a ferrofluid droplet to encapsulate cargo inside, enabling cargo collection, transportation and targeted release, Figure 9b.

Compared to bare droplets in the air, the addition of magnetic particles of LMs can combine with the fabrication of their particle shells. Hence, the introduction of magnetic components is no longer restricted to the interior of the droplet and can also be accomplished by modifying the particles on a liquid–air interface. This feature reduces the risk of cross-contamination of the sensitive liquid core and greatly expands the inner space of LM-based microreactors. Certainly, the balance of forces still needs to consider, ensuring the driving force is sufficient to defeat the motion resistance but the magnetic particles do not break away from the surface at the same time. Zhao et al. have demonstrated the feasibility of magnetic actuation for LMs [121]. They synthesized magnetic LMs using hydrophobized Fe_3O_4 nanoparticles and then realized the transferring of LM through a magnet bar, Figure 9c. Xue and his team further explored the possibility of magnetic LMs acting as microreactors by combining magnetic nanoparticles with fluorinated decyl polyhedral oligomeric silsesquioxane, stabilizing the LM prepared by low surface tension liquid [122]. The movement of LMs on a liquid surface can also be driven by a magnetic field, which was demonstrated by Khaw and co-workers, Figure 9d [99]. In addition, due to their low friction and high stability, LMs outperform droplets when driven by gravity on the magnetically responsive material substrate, Figure 9e [123]. This way utilized the magnetically responsive materials directly as a broad liquid substrate, eliminating the need for troublesome machining of magnetically responsive microspheres.

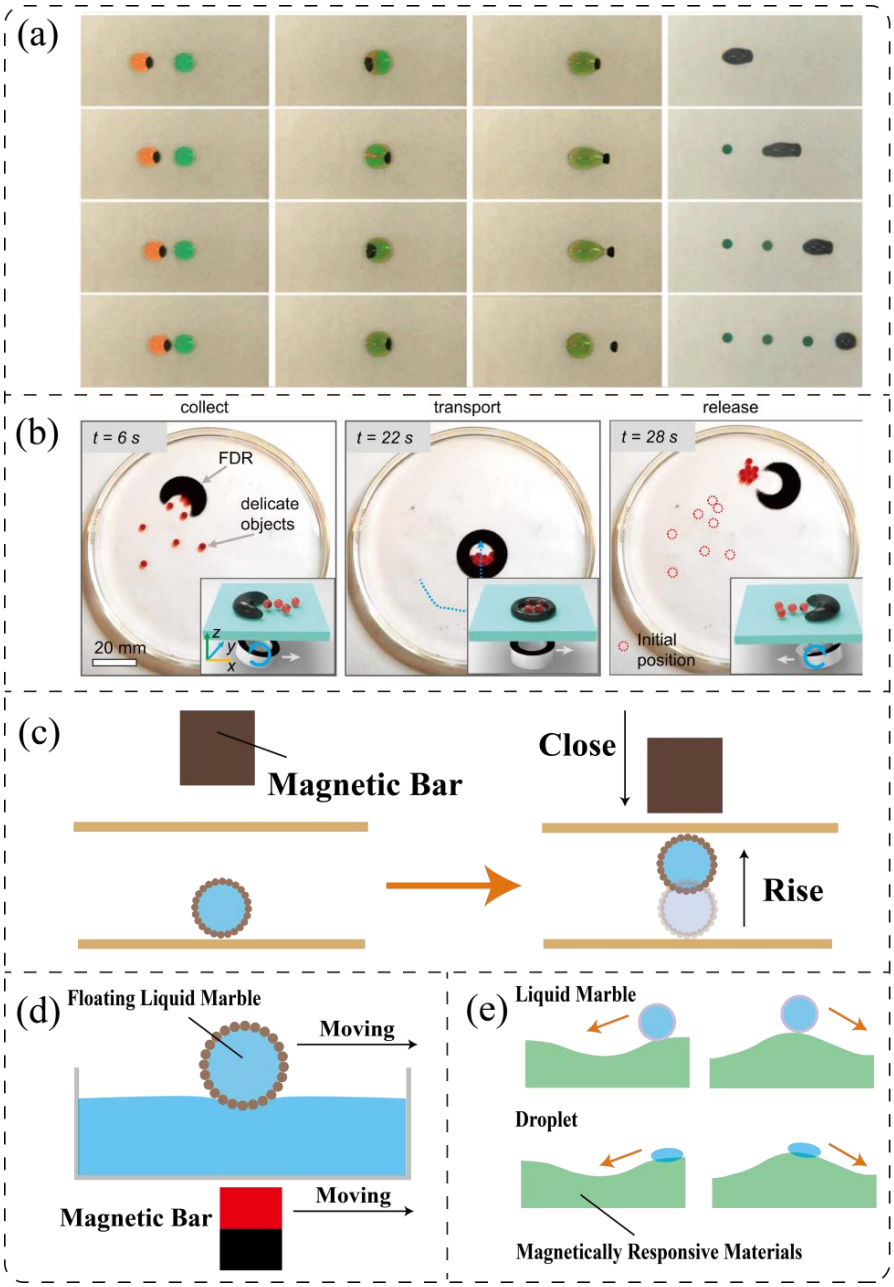

Figure 9. (**a**) The transportation, fusion, mixing, MPs extraction and dispensing of droplets containing magnetic particles [116] (Reproduced with permission from John Wiley and Sons, 2013). (**b**) Snapshots of ferrofluid droplets that collect, transport and release delicate objects [120] (Reproduced with permission from PNAS, 2020). (**c**) Schematic diagram of transferring LMs between two parallel plates by a magnetic bar [121]. (**d**) Schematic of the movement of magnetic LMs on the water surface [99]. (**e**) Schematic diagram of the motions of LMs and droplets on a controllably magnetic deformed substrate [123].

3.2.3. Acoustic Field

Compared to the electric and magnetic fields, the acoustic field shows fewer limitations on the property of target objects. This is due to the transfer of acoustic energy being simpler and much more direct. Theoretically, acoustic waves can inspire any object within their effective range. Reasonable control of the active form of acoustic waves can precisely work on the motion of bare droplets. In 2004, researchers first used lithographic techniques to modify the surface hydrophobicity for creating virtual tracks and successfully confined

the droplet motion induced by surface acoustic waves in these tracks, Figure 10a [102]. Subsequently, based on a slanted finger interdigitated transducer, Bourquin et al. controlled the movement direction of droplets by regulating the action position of surface acoustic waves, Figure 10b [124]. In addition, surface acoustic waves could also be used to indirectly trigger the movement of droplets. By the action of the surface acoustic wave, the continuous phase fluid would continuously drive the discrete phase droplets on its surface to the capture zone [83]. Recently, a more exciting work was presented by Yang's group. Here droplets were restricted on a PTFE thread and driven by the sound sources on either side of the droplets, rather than the common surface acoustic waves [125].

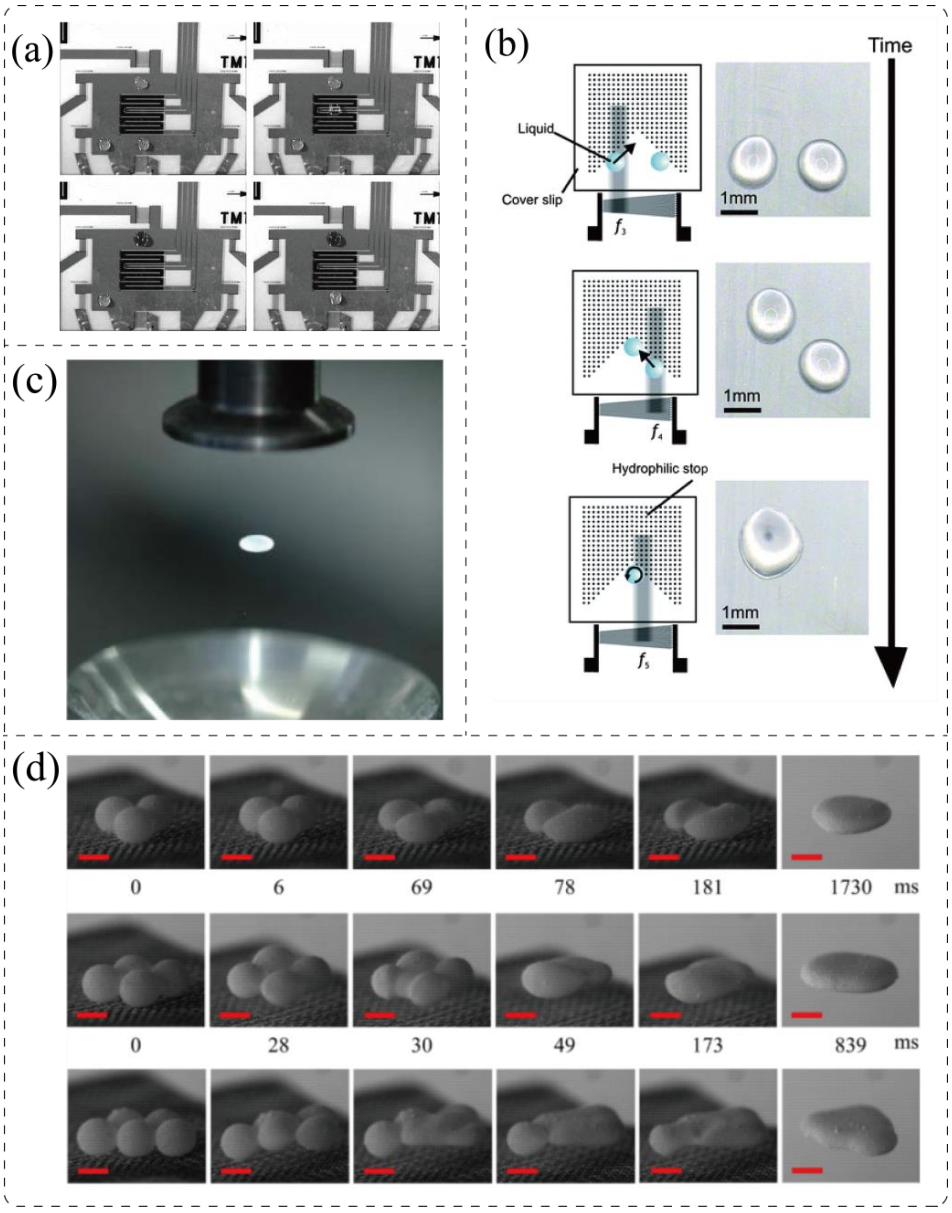

Figure 10. (**a**) Snapshots of droplets moving along a pre-designed track for merging under the action of surface waves [102] (Reproduced with permission from Springer Nature, 2004). (**b**) Two droplets with different orientations merge at specific positions under the asymmetric action of surface acoustic waves [124] (Reproduced with permission from Royal Society of Chemistry, 2010). (**c**) An LM is levitated by sound waves [126] (Reproduced with permission from American Chemical Society, 2015). (**d**) The levitation and coalescence of multiple LMs in a sound levitator (scale bar: 2 mm) [127] (Reproduced with permission from American Chemical Society, 2017).

Similarly, acoustic-field actuation is also a remarkable way in LMs transportation. At the same time, the properties of LMs permit more operation opportunities and perform better in acoustic actuation. For instance, the high stability of LMs allows them to safely suspend in an acoustic levitator, providing a convenient way to transport LMs, Figure 10c [126]. Acoustic-field actuation is not limited by the number of LMs within a certain working range, and thus this means is quite effective for triggering multiple LMs to collide and merge with each other, Figure 10d [127]. In addition, the particle shell can also be redistributed under the appropriate action of the acoustic field, a feature that permits the LM to be opened like a handy toolbox only when in service. However, there is also a risk for the acoustic manipulation process, which is that it may break up if the field strength is excessively strong, especially in the open air.

3.2.4. Optical Field

Optical-field actuation is generally not as direct as electric, magnetic, or acoustic fields in driving droplets or LMs. This actuation approach heavily relies on light-responsive materials. Moreover, optical actuation usually requires a light transmissive environment, and the heat load accompanying the light field will accelerate the evaporation rate of the liquid, which may sharply shrink the service period of small-volume liquid. However, this approach is a remote, contactless and indirect actuation way, without the limitation on the working path in an open environment. Azo–benzene molecules are one of the most classical photosensitive materials that can undergo photoisomerization. When irradiating an azo–benzene molecule with UV light, the molecule becomes cis-isomeric with a higher surface free energy. Conversely, irradiation with blue light reverses the cis-isomer to a trans-isomer with a lower surface free energy. Based on this, Ichimura's team used this material to modify the substrate surface and successfully shifted droplets by adjusting the related optical field, Figure 11a [128]. With advances in materials technology, more materials with photothermal-response properties have been developed and applied for actuating droplets. Hwang et al. introduced polypyrrole nanoparticles covered by N-vinyl pyrrolidone dispersions into a 10-µL droplet to improve its photothermal properties [129]. When the droplet was irradiated with a near-infrared laser, the temperature of the irradiated region increased. As the temperature changed, a surface tension gradient was formed at the droplet-air interface, which in turn led to the formation of an internal Marangoni flow, causing the droplet to move immediately, Figure 11b. Although LMs cannot be driven on the solid substrate modified by light photoisomerization molecules, their unique properties inspire more explorations in controlled optical manipulation. Chu et al. proposed a convenient and long-range method for manipulating LMs [26]. In their work, the $CHCl_3$ LMs encapsulated by photothermal nanoparticles could stably stay in the water. Under the irradiation of a near-infrared laser, the photothermal nanoparticles emitted a large amount of heat, which vaporized $CHCl_3$ and formed air pockets. Subsequently, the LMs gradually float up from the bottom as the airbag grew, making the LMs a maneuverable platform in the water. Further adjustment of the laser irradiation enables the LMs to ascend, shuttle, suspend or even horizontal movement inside the liquid, Figure 11c.

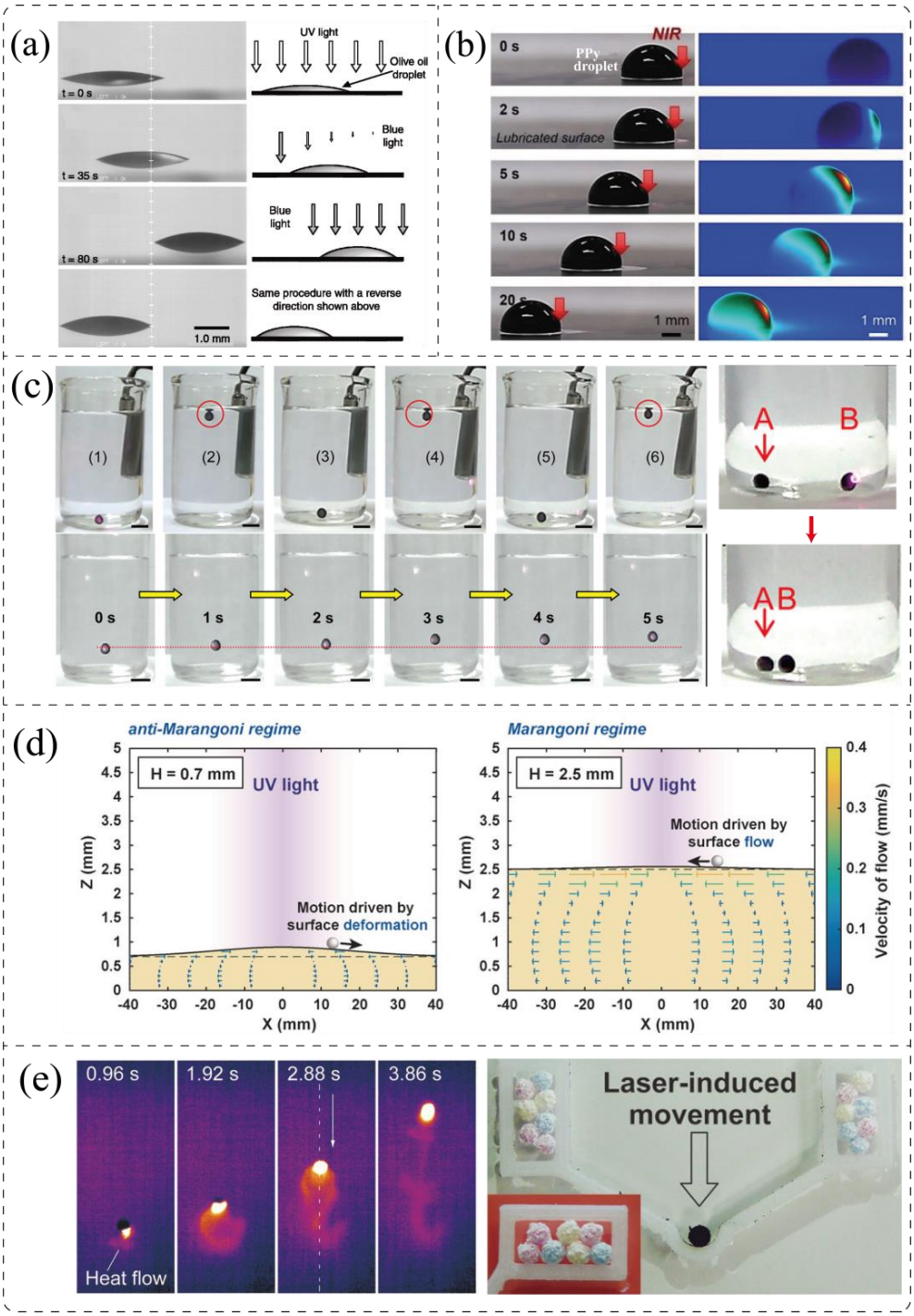

Figure 11. (**a**) The motion of an olive oil droplet on a silica plate modified with CRA−CM, due to the asymmetrical irradiation [128] (Reproduced with permission from The American Association for the Advancement of Science, 2000). (**b**) PPY droplet motions on a lubricated surface by NIR irradiation [129] (Reproduced with permission from John Wiley and Sons, 2022). (**c**) The shuttling process in three cycles numbered from (1) to (6), the short-period suspending and the horizontal movement of an LM in liquid controlled by a laser [26] (Reproduced with permission from American Chemical Society, 2016). (**d**) The Marangoni regime and anti-Marangoni regime motions of LMs [130] (Reproduced with permission from John Wiley and Sons, 2016). (**e**) Snapshots of the light-driven LMs observed by thermography and the delivery of materials and objects by a light-driven LM [25] (Reproduced with permission from John Wiley and Sons, 2016).

Interestingly, photosensitive materials are not only feasible for modifying solid substrates but also for liquid carrier surfaces, which in turn provides more options for the transportation of LMs on a liquid surface [103]. Furthermore, LMs can stably remain spherical on liquid, a feature that endows them with unusual dynamic behaviors when moving. For example, LMs may show anti-Marangoni flow movements on the surface of an aqueous solution containing surfactants [130]. The reason is that when the liquid thickness is less than the threshold value, the region irradiated by UV light undergoes a significant deformation, due to the accumulation of Marangoni flow. Thus, an LM will move against the Marangoni flow under the effect of gravity. When the liquid thickness is larger than the threshold value, the deformation caused by the UV light irradiation is not enough to actuate the LMs in the opposite direction, Figure 11d. In addition, the dynamic behavior of LMs on a liquid surface can be controlled by the temperature gradient in its vicinity, as long as the difference in surface energy based on temperature difference is significant enough. For instance, when the near-infrared light was shone on one side of the LM prepared with photothermal powders, the temperature of the particles on the water surface increased rapidly and the nearby liquid was heated [25]. This asymmetric heating would cause a surface tension gradient in the liquid on both sides of the LM, which created a driving force strong enough to drag cargo, Figure 11e.

4. Other Manipulation Tasks of Bare Droplets and Liquid Marbles

While reliable transportation lays the basis for small-volume liquid manipulation, coalescence is critical to release more functions of these independent systems in OMF such as microreactors, microsensors and microincubators. Following this, mixing is another important manipulation task for microreactions in various droplets or LMs, where the induced microscale flow can bring a few reagents into contact on purpose. The splitting of droplet samples is also one good example of the diversity of controlled liquid manipulation, which has an immeasurable potential for applications in split-sample tests and microbial culture. Coalescence is an easy task for bare droplets and merge naturally upon touching each other. However, for LMs, coalescence is tough even though the subsequent merging process after a liquid–liquid connection is consistent with that of droplets, Figure 12a [131]. There usually exists an obstacle of protective particles that need to be overcome, when an LM merges with either a droplet or another LM. As described, adequate mixing allows for the full contact of biochemical components within the liquid content, shortening the related reaction time dramatically. As liquid-based microreactors with 3D interior space, droplets and LMs can be well mixed in a simple way, such as stirring or shaking. Splitting is the liquid separation of daughter bodies from their parent counterpart, an operation often used for waste disposal. The methods of splitting for droplets and LMs have much in common, although LMs require more energy to break the particle shell. However, the presence of the particle shell also endows LMs with some unique splitting methods.

4.1. Coalescence

There are two main forms of coalescence for sessile droplets. One drives two sessile droplets to contact each other, and the other is to add a free drop directly over a sessile droplet. In either form, the coalescence of droplets begins with contacting simultaneously. During the contact process, a thin air film between two droplets will be broken. Then a liquid neck connecting the droplets will emerge and gradually expands under the control of Laplace pressure until the merging process completes [132]. Considering this, most of the transportation methods mentioned in the above section could effectively trigger droplet coalescence, for instance, wettability gradients, electric, magnetic and acoustic fields, as well as the Marangoni flows. Among these methods, the Marangoni flow seems more straightforward and unique. When two composite droplets containing liquids with different evaporation rates and surface tensions are near proximity, these droplets attract each other and coalesce. Moreover, the coalescence based on concentration differences is selective and only occurs when their concentrations are similar, Figure 12b [89].

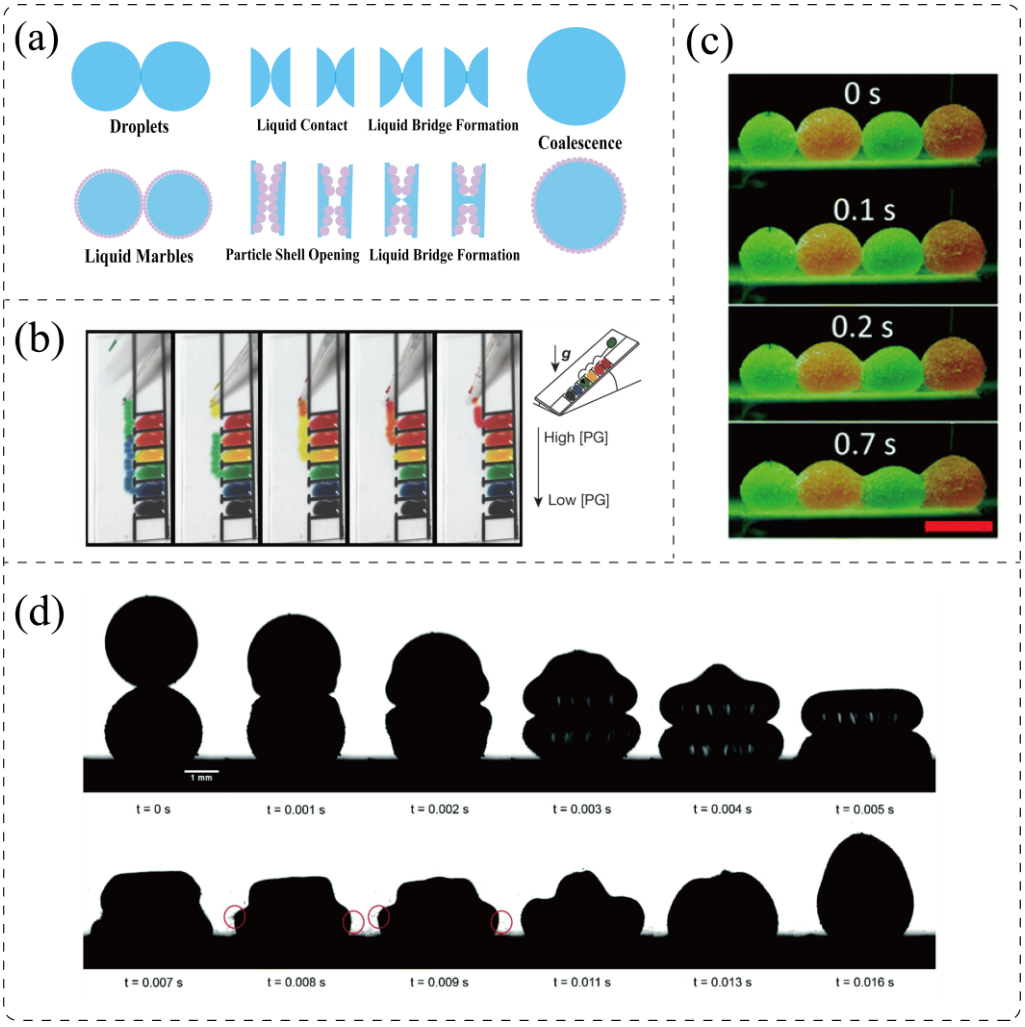

Figure 12. (**a**) The coalescence processes of droplet-to-droplet and LM-to-LM. (**b**) The merging of droplets with a similar concentration after passing through other droplets under gravity [89] (Reproduced with permission from Springer Nature, 2015). (**c**,**d**) Different fusion processes of LMs under the action of electric force and gravity, respectively. The red circles outline the particle aggregates ejected in vertical marble collisions [133,134] (Reproduced with permission from Royal Society of Chemistry, 2017 and 2018, respectively).

The presence of a particle shell in LMs is the most essential distinction from bare droplets, isolating the liquid core from the outsides and extensively protecting LMs from external contamination. However, this rounded protection becomes a major impediment to the coalescence of LMs, confining the penetration of extra reagents, which is not expected when LM-based miniaturized vessels are applied. In order to explore the great potential of LMs, it is necessary to use external forces to break up the physical barrier of solid particles before forming a liquid–liquid bridge. After the liquid–liquid contact, LMs will spontaneously merge as the whole system evolves towards the minimum surface energy. The use of an electric field can easily climb over energy barriers and may even break several solid shells together to complete the coalescence of multiple LMs. Liu et al. have investigated the phenomenon of LM coalescence with a direct current [133]. Under the action of the direct current, the contacting marbles were deformed at the liquid–liquid interface and a conical tip inside the particle shell was formed. Then a liquid connection bridge appeared when the deformation was sufficient, followed by the growth of this bridge in the rest coalescence process, Figure 12c. The threshold voltage for this coalescence is affected by the particle size and the surface tension of the liquid core and increases linearly with the number of LMs.

It was found later that the severe deformation by collisional squeezing can also construct liquid bridges to promote LM coalescence. Jin and co-workers systematically studied the vertical collision-induced merging of two LMs [134]. When the upper LM collided with the bottom LM with a certain kinetic energy, both LMs would be deformed and internal flows occurred. The strong internal flow allowed the particles around the contact region to move rapidly to the periphery and formed an opening liquid neck simultaneously. Then, the coalescence process was accomplished as the liquid neck grew entirely, with the ejection of extra particles, Figure 12d. Furthermore, sounds can be utilized as an available energy source to remove the physical hindrance to LM coalescence [127]. Interestingly, the connection between LMs under the action of an acoustic field may occur before the main body collision, and even the liquid cores of LMs remain isolated after contact. It was believed that this phenomenon was closely related to the intensity of the sound. When the sound intensity was weak, the liquid cores of suspended double LMs in the air may even keep isolated without merging into a bigger LM, even if the acoustic field continued to work.

The controlled opening and closing of the particle shell is one of the most popular features of LMs, and its implementation creates infinite possibilities for the operation and application of functional LMs. For example, during the shell opening period, reagents can be added to target LMs arbitrarily. While the shell is closed again, it can continue to protect the liquid core from external disturbances. However, opening and closing the particle shell is still a challenging task, which strongly relies on external assistances, and the most commonly used ones are magnetic and acoustic fields, Figure 13a–c [121,122,126]. Fortunately, Rozynek and co-authors have recently proposed a different approach to open and close the particle shell of an LM, expanding the choices to control the particle shell [135]. This group put the droplet with fully covered particles into an electric field. Initially, the electrohydrodynamic flow was suppressed, due to the weak electric field, the small droplet deformation and the tightly arranged particle layer. As the electric field strengthened, the droplet deformation increased and the surface particles tended to detach. At this point, the electrohydrodynamic flow started to occur and the particles began to move, forming an opening area in the electric pole of the droplet. Finally, as the electric field strength gradually decreased until it disappeared completely, the opening area healed, Figure 13d. This method demands little particle properties and is suitable for droplets covered with magnetic or nonmagnetic particles, which can be used more widely in biochemical analysis.

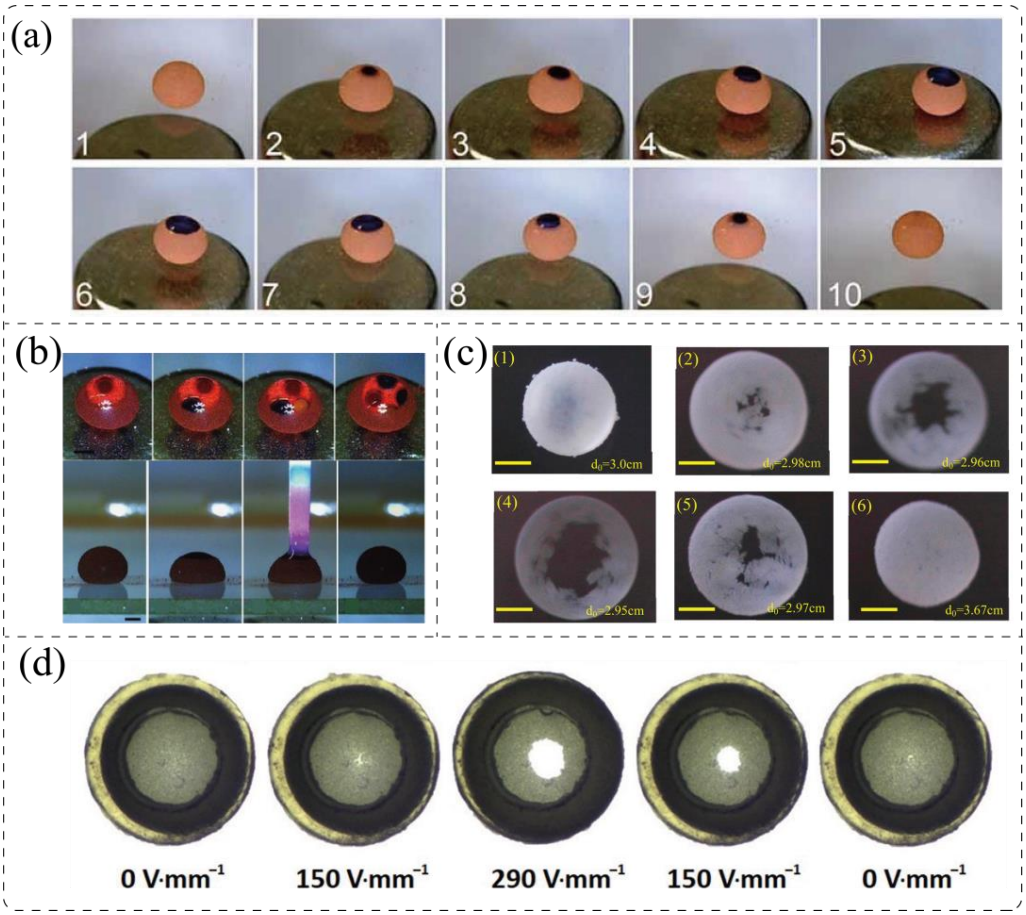

Figure 13. (**a**) Snapshots of the opening and closing of particle shells in LMs under a magnetic force [121] (Reproduced with permission from John Wiley and Sons, 2010). (**b**) The regent addition and chromatographic analysis in an opened magnetic LM [122] (Reproduced with permission from John Wiley and Sons, 2010). (**c**) Opening and closing of particle shells under the action of an acoustic field [126] (Reproduced with permission from American Chemical Society, 2015). (**d**) Opening and closing of particle shells under the action of an adjustable electric field [135] (Reproduced with permission from American Chemical Society, 2019).

4.2. Mixing

The purpose of mixing is to reduce the time consumption of multiple reactions in droplet microsystems. By accelerating the internal flow of liquid and promoting different liquid components to come into contact with each other, a faster reaction rate can ultimately be achieved. Fortunately, due to the viscosity of a liquid, even simple fluctuations can induce the occurrence of internal flow in droplets or LMs [136,137]. At present, to further reduce the time consumption of various reactions, several strategies that can greatly enhance the mixing effect have been developed. For instance, Wang et al. controlled two different wetting states of a droplet on the superhydrophobic surface by adding and removing an electric field, Figure 14a. The fast switching of droplet states could accelerate the internal flow inside the droplets, which was capable of shortening the complete hybridization of DNA from 12 min to only 10 s [138]. Yang et al. used an electrode needle to control the magnetic beads inside a droplet, which achieved a similar mixing acceleration [117]. The repeated movement of the electrode needle on the droplet surface drove the movement of the magnetic beads, leading to the internal liquid flows, Figure 14b. Li's team further simplified the method of using a magnetic field to control and promote the internal flow of droplets, with only two steel beads instead, Figure 14c [100]. Won and co-workers have proposed another approach to enhance the mixing effect in droplets by adopting sound fields, Figure 14d [139]. Under the stimulation of a piezoelectric actuator, microflows would be generated in the vicinity

of the bubbles inside the droplet, promoting the mixing of the internal components. This method significantly improves the mixing performance of droplets on open surfaces. In addition, the direct use of electric fields in LMs is also effective in triggering the mixing process inside and reducing the related reaction time. For example, Liu et al. systematically investigated the effect of an electric field on LM coalescence and mixing. Under electric fields, they have observed an obvious mixing acceleration phenomenon in the micro reaction process inside LMs, Figure 14e [140]. The reaction of 2-methylindole and aldehyde with the assistance of an electric field was completed in 6 s, while the traditional heating method still took at least 12 min to finish.

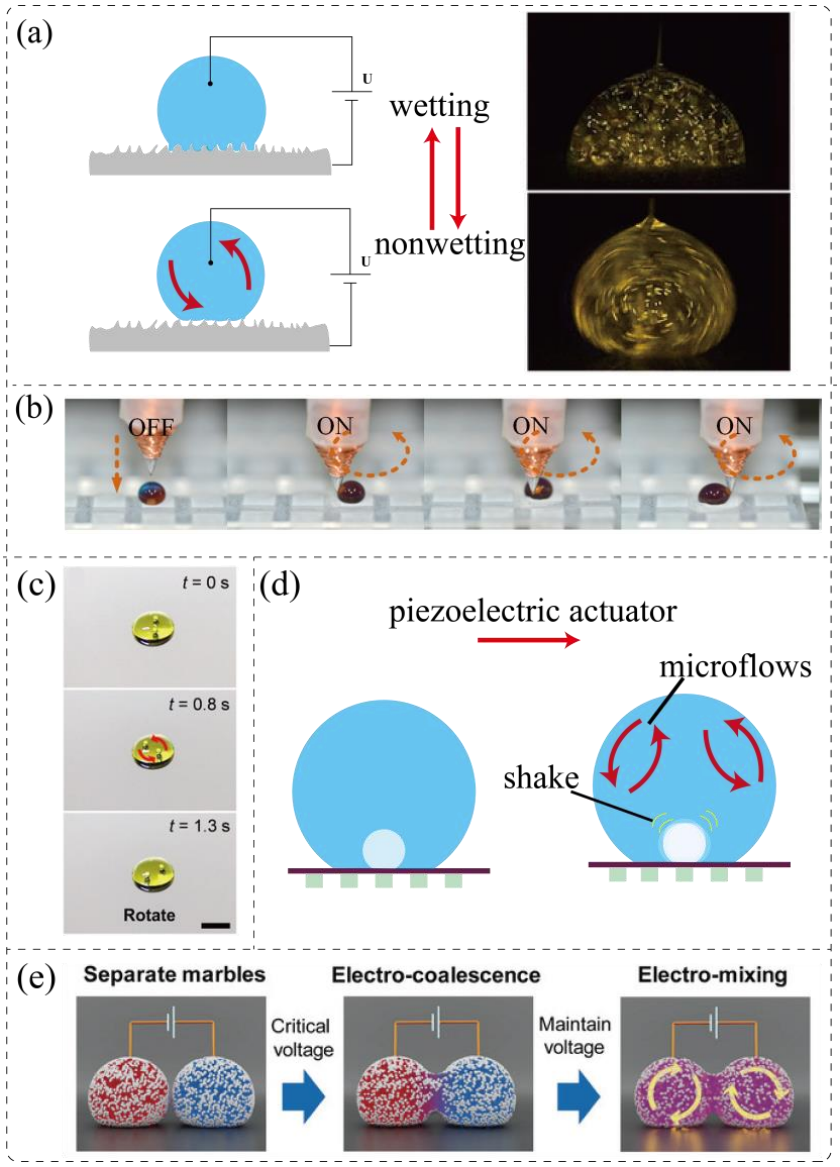

Figure 14. (**a**) The mixing is caused by the switching of droplets between wetting and nonwetting states [138] (Reproduced with permission from Springer Nature, 2008). (**b**,**c**) Acceleration of mixing in droplets caused by the internal rotation of magnetic particles [100,117] (Reproduced with permission from Elsevier, 2017; American Association for the Advancement of Science, 2020). (**d**) The efficient mixing is assisted by acoustic bubbles [139]. (**e**) The detailed process of LMs from the separate state, coalescing state until mixing state, under a well-controlled electric field [140] (Reproduced with permission from John Wiley and Sons, 2019).

4.3. Splitting

Coalescence corresponds to the foundation of the droplet-based microreactor, while splitting is key for the microincubators to maintain the optimal conditions for cell culture. For splitting, it is necessary to have a continuous force to keep the liquid deformed until full separation. Luckily, droplets, as a soft microsystem, require a quite small force for deformation, so there are many options available for droplet splitting. Electricity has always been extraordinary in controlled droplet manipulation, and the electrowetting phenomenon is representative of this. In EWOD, the quick energization of the electrode under a droplet can finely regulate the droplet's surface tension, and this characteristic can be exploited to create a surface tension gradient near the droplet. The lasting effect of the surface tension gradient can continuously force the droplet to deform until the droplet is separated into two smaller droplets, Figure 15a [141]. Moreover, this method is also valid in distributing multiple sub-droplets from a large droplet. Not surprisingly, the use of a magnetic field is another effective means to assist the splitting operation. For example, Zhang et al. fabricated high surface energy regions on a low surface energy Teflon membrane as traps, smoothly completing the droplet dispersion with the assistance of a magnetic field [116]. In this work, when the original droplet passed through the traps, the majority of droplets kept moving and the minority of droplets were left in the traps. Gravity, although non-adjustable, still shows great potential for separating droplets. Accordingly, Mertaniemi's team prepared superhydrophobic blades on an inclined superhydrophobic track. When a droplet moved along the direction of the gravitational gradient, it was split into two parts by the pre-set superhydrophobic blade above because of strong impacts, Figure 15b [142]. Additionally, Song's group has fabricated specific superhydrophobic strips on hydrophilic surfaces to achieve droplet splitting. When droplets fell and impacted the superhydrophobic strip, the surface tension in the hydrophilic region would stretch the droplet outward and thus prevent the contraction of the three-phase contact line. By contrast, the surface tension on the superhydrophobic strip would like to pull the droplet inward. Finally, under the surface tension of different directions, the droplet appeared to look like being cut with a blade, Figure 15c [143].

As aforementioned, the particle shell of LMs has not only increased the difficulty of merging but also raised the energy requirement for their splitting operation. However, the particle shell is not always a hindrance to LM splitting. The high stability brought by the protection of the particle shell permits the separation of LMs to be executed in a wilder way. For example, the splitting of LMs can be easily done with a solid rod or even just with a finger, Figure 16a [70]. Furthermore, this high stability of the particle shell facilitates the LM to be split in more accessible ways. For instance, Bormashenko et al. have discovered that under the protection of the particle shell, the LM was able to exist stably in the oil phase and jetting can occur in the oil. This is because Taylor instability appeared when LM submerged in oil suffered a sufficiently large DC field, forming a cone and ejecting tiny droplets, Figure 16b [97]. As the DC field can be properly controlled, it is regarded as an effective method to split LMs. In addition, Wang's team presented a device to ensure that LMs serving as 3D cell culture platforms stay in an optimal cellular microenvironment over time [144]. Among multi-channels with different functions, the working principle of splitting channels is quite interesting and simple. The splitting of LM is achieved by gravity through setting copper wires on the falling path of LMs, Figure 16c. More conveniently, the size of the sub-LM can also be controlled by adjusting the position of the copper wire. In most cases, the main body of LM protected by a stable particle shell has less mass loss in splitting, unlike excessive splashing of droplets. Generally, the number of particles is enough to wrap around the two liquid droplets after harmless splitting. In this channel, the removal of waste liquid from the culture solution can be thus easily realized by marble splitting.

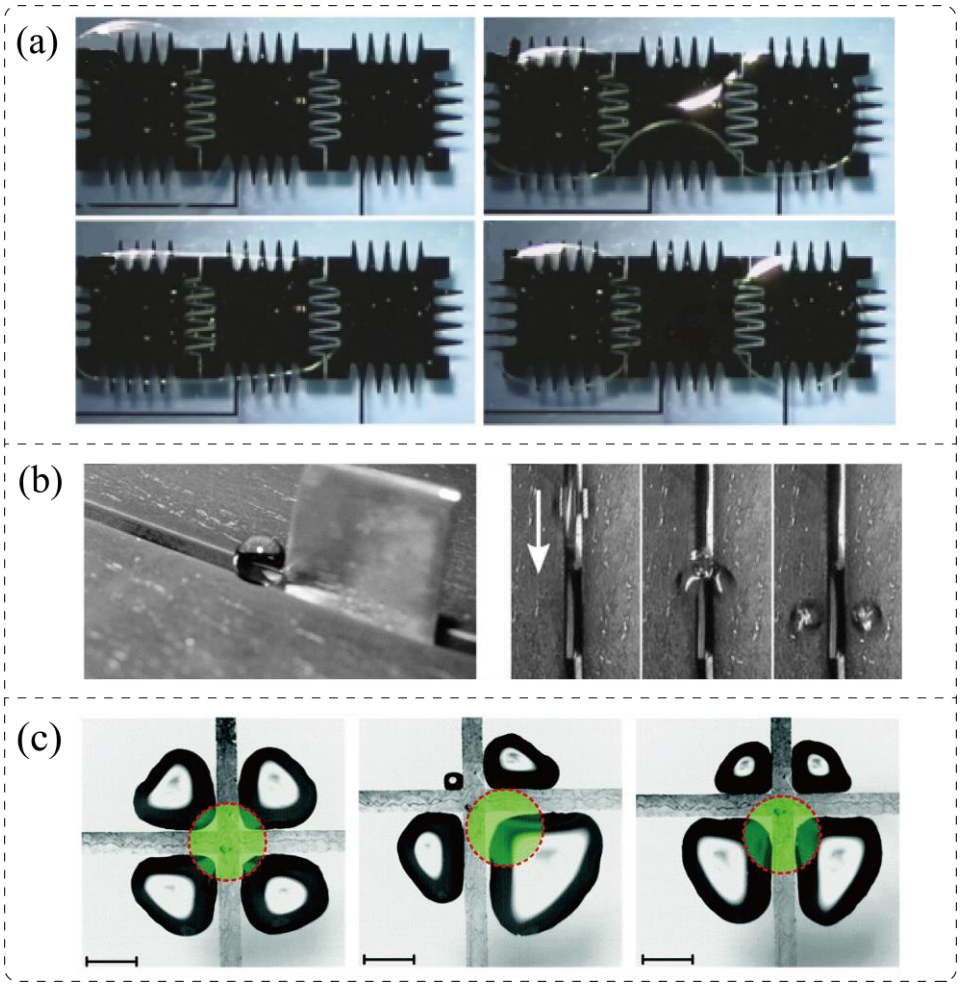

Figure 15. (**a**) Separation process of liquid droplets by electrode switching [141] (Reproduced with permission from Royal Society of Chemistry 2002). (**b**) Schematic of gravity-actuated droplets being divided into two parts by a superhydrophobic knife [142] (Reproduced with permission from John Wiley and Sons, 2011). (**c**) The snapshots of a big droplet split into multiple small droplets by superhydrophobic stripes. The green shadows circled by red dots show the size and initial landing position of the big droplet, with a scale bar of 2 mm [143] (Reproduced with permission from the Royal Society of Chemistry, 2015).

Actually, it is common sense that either droplets or LMs have a spherical appearance of their daughter after splitting, because spherical condensed matter tends to have the smallest surface area. However, Liu et al. found some unusual phenomena in their recent study, where LMs did not spontaneously become sphere-like shapes after being cut, but could be deformed randomly and even shaped into English letters on demand [145]. The authors pointed out that this behavior was attributed to the particle surface density. When the particle surface density is small, the behavior of LMs is closer to liquid droplets. And when the particle surface density is large enough, its behavior is more like a solid. Therefore, cutting and separating the LMs with higher particle density is more accessible, just like cutting a pudding in life, Figure 16d.

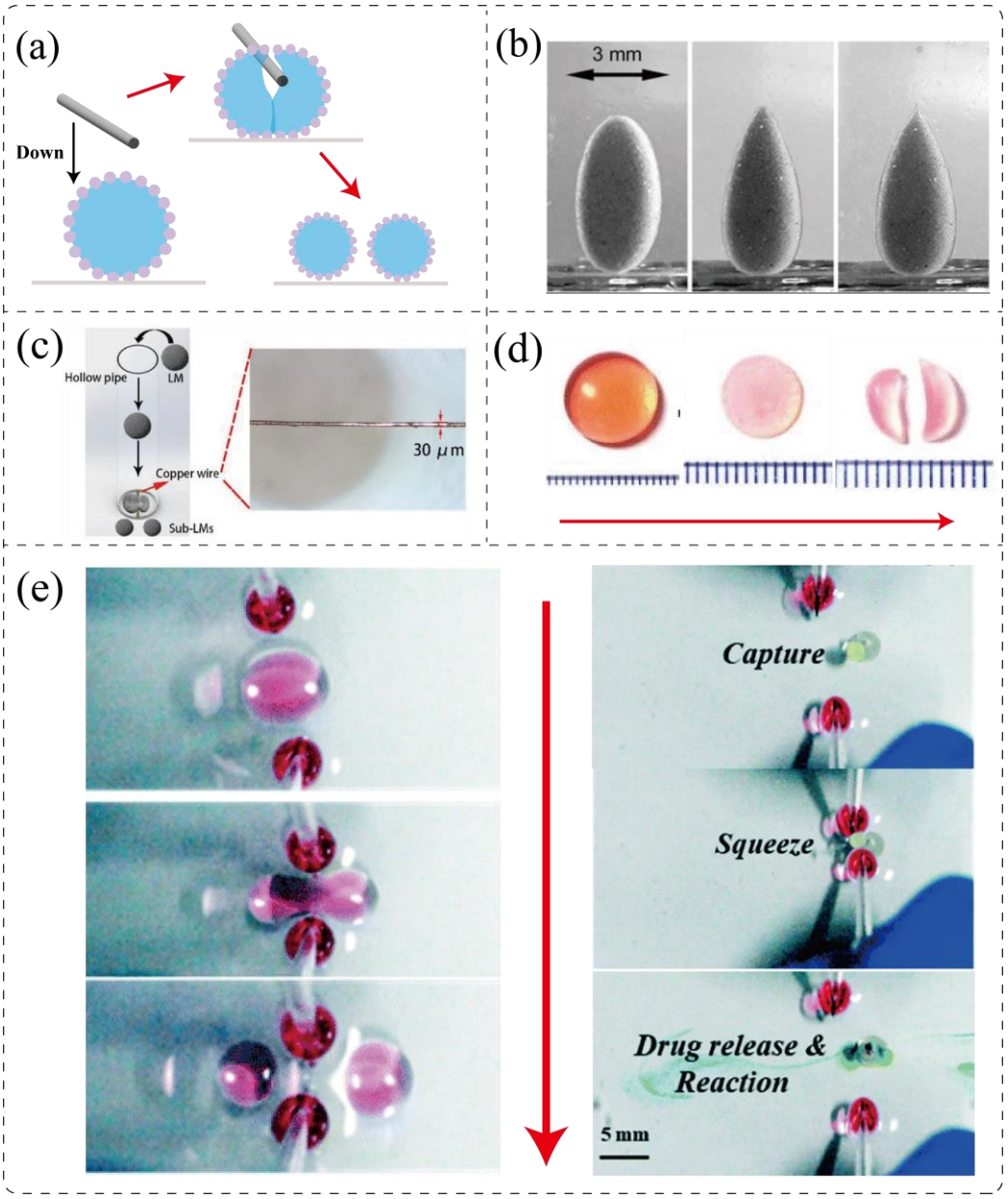

Figure 16. (**a**) Division of a water marble by a solid rod [70]. (**b**) Lycopodium-coated marble deformed in an electrostatic field to a Taylor cone and the related jetting [97] (Reproduced with permission from Springer Nature, 2013). (**c**) An LM is split into two daughter LMs, caused by a copper wire during the fall process [144] (Reproduced with permission from John Wiley and Sons, 2019). (**d**) An LM is cut into two portions that are not like the traditional spherical cap [145] (Reproduced with permission from Springer Nature, 2016). (**e**) The droplet splitting, accurate transport and release on demand of LMs, under the decanol liquid lenses action [146] (Reproduced with permission from Royal Society of Chemistry, 2022).

In the above section focusing on transportation, a method for transporting small-volume liquid based on concentration gradients was introduced. Recently, Yang et al. proposed a similar strategy for droplet splitting and the targeted bursting of LMs by using the concentration gradient [146]. They added two droplets of decanol to an aqueous solution to act as decanol liquid lenses and operated them with a polypropylene pipette tip. Since decanol is slightly soluble in water and its concentration decreases radially along the liquid−air interface of the decanol liquid lens, a surface tension gradient field is formed around it. As the decanol liquid lens approached the target droplet, an asymmetry surface tension

would raise around the droplet, leading to the motion of the target droplet. Furthermore, droplet launching can be achieved when two decanol liquid lenses get close to each other from the tails of the target droplet separately. When the lenses move together along the axisymmetric line of the target droplet to the center, droplet splitting can be realized and this manipulation scheme also enables point splitting of LMs to release different drugs, Figure 16e.

5. Conclusions and Perspectives

As two promising independent platforms in OMF, bare droplets on solid substrates, especially on superhydrophobic surfaces, as well as LMs, no matter in air or liquid and on solid carriers, have attracted more attention among international researchers in the fields from life science to industrial engineering. In this review, we have comprehensively discussed recent studies of bare droplets and LMs, from the perspectives of unique features, formation mechanisms, and actuation principles to applied techniques in operation. Considering the exciting advantages and rapidly evolving operational approaches of both novel OMF platforms, this review also aims to offer a snapshot for those who are interested in the fundamentals and applications of small-volume droplet systems. It is worth noting that the porous protective particles, often hydrophobic, enrich the manipulation of LMs and thus empower LMs to have more functions in versatile applications.

A large number of theoretical studies claim the hindrance of driving droplets and LMs on solid surfaces due to the liquid viscous dissipation. Although experimental results with minor differences rightly substantiate this claim, more details on droplets and LMs should be considered. Numerous works have studied the motion of LMs on solid surfaces by treating them as droplets on superhydrophobic surfaces, but this analysis fails to take into consideration the difference between discrete particles and continuous solid substrates. More efforts are needed to identify this difference for understanding the motion mechanism of LMs better, which lays the foundation for future applications of LM-based microreactors.

As for manipulation, both droplets and LMs can be effectively manipulated for various tasks under the appropriate action of an external field. In particular, there are some distinctive operations of LMs due to the protection brought about by the solid particle shell. For example, the transportation on or below the liquid surface and the controllable opening and closing of the particle shell. In general, the absolutely isolated liquid core of LMs cannot interact directly with the external environment. This results in LMs losing the flexibility to sense the external wettability as well as tiny structural changes. Therefore, LMs cannot be driven like droplets by adopting the wettability gradient resulting from the solid surface modification. However, as hydrophobic particles show less friction on various substrates, LMs usually experience less resistance in controlled actuation, especially on the liquid surface. Moreover, LMs prepared with single-layer nanoparticles, as a special case in the marble family, seem to differ from conventional LMs. They are still able to temporarily possess the ability to sense the external environment inside the solid surface when certain conditions are met. This particular LM needs more investigation in the future to develop its potential applications. Among other manipulation tasks, the particle shell seems to be an obstacle to achieving the operation. For instance, in the process of LM merging, the extra energy required by the particle shell makes the corresponding merging operation much more difficult. Nevertheless, the high stability resulting from the particle shell provides some convenience to the splitting operation, allowing for a wilder approach and effectively reducing unnecessary liquid splashing during the splitting process.

In summary, bare droplets and LMs, as essential components in OMF systems, demonstrate plenty of excellent properties. They have great potential in serving as multifunctional microreactors, which provides more options for versatile liquid-based applications in many fields ranging from life sciences to industrial engineering. However, there is still a long way to go before large-scale commercial use of LMs can be achieved. More details, for instance, the stability and lifecycle of LMs with different coating particles should be further

investigated and more cross-disciplinary applications should also be actively explored in the near future.

Author Contributions: Conceptualization, Z.H. and J.J.; Methodology, Z.H., Y.X. and J.J.; Validation, Z.H. and Y.X.; Investigation, Z.H.; Writing—original draft preparation, Z.H. and J.J.; Writing—review and editing, Z.H., Y.X., H.C., Z.Y., L.S. and J.J.; Visualization, Z.H.; Supervision, J.J.; Project administration, H.C., L.S. and J.J.; Funding acquisition, J.J.; All authors have read and agreed to the published version of the manuscript.

Funding: This research was funded by the National Natural Science Foundation of China (grant number: 62204070), Guangdong Basic and Applied Basic Foundation (grant number: 2020A1515110901 & 2022A1515010054), and Shenzhen Science and Technology Innovation Committee (grant number: GXWD20220811151610001).

Data Availability Statement: Not applicable.

Acknowledgments: The authors appreciate the support from School of Mechanical Engineering and Automation, Harbin Institute of Technology, Shenzhen and University Town Library of Shenzhen for their resources. The authors acknowledge the financial support by National Natural Science Foundation of China, Guangdong Basic and Applied Basic Foundation, and Shenzhen Science and Technology Innovation Committee.

Conflicts of Interest: The authors declare no conflict of interest.

References

1. Manz, A.; Graber, N.; Widmer, H. Miniaturized total chemical analysis systems: A novel concept for chemical sensing. *Sens. Actuators B Chem.* **1990**, *1*, 244–248. [CrossRef]
2. Woolley, A.T.; Mathies, R.A. Ultra-High-Speed DNA Sequencing Using Capillary Electrophoresis Chips. *Anal. Chem.* **1995**, *67*, 3676–3680. [CrossRef] [PubMed]
3. Sreejith, K.R.; Ooi, C.H.; Jin, J.; Dao, D.V.; Nguyen, N.-T. An automated on-demand liquid marble generator based on electrohydrodynamic pulling. *Rev. Sci. Instrum.* **2019**, *90*, 055102. [CrossRef] [PubMed]
4. Wang, Y.; Cui, C.; Qi, B.; Wei, J.; Zhang, Y. Study of droplet self-migration on silicon surface with radial micro-fin structures. *Exp. Therm. Fluid Sci.* **2020**, *114*, 110075. [CrossRef]
5. Lv, J.-A.; Liu, Y.; Wei, J.; Chen, E.; Qin, L.; Yu, Y. Photocontrol of fluid slugs in liquid crystal polymer microactuators. *Nature* **2016**, *537*, 179–184. [CrossRef]
6. Lei, W.; Hou, G.; Liu, M.; Rong, Q.; Xu, Y.; Tian, Y.; Jiang, L. High-speed transport of liquid droplets in magnetic tubular microactuators. *Sci. Adv.* **2018**, *4*, eaau8767. [CrossRef] [PubMed]
7. Sackmann, E.K.; Fulton, A.L.; Beebe, D.J. The present and future role of microfluidics in biomedical research. *Nature* **2014**, *507*, 181–189. [CrossRef]
8. Elvira, K.S.; i Solvas, X.C.; Wootton, R.C.; Demello, A.J. The past, present and potential for microfluidic reactor technology in chemical synthesis. *Nat. Chem.* **2013**, *5*, 905–915. [CrossRef]
9. Qiu, Y.; Liu, Y.; Xu, Y.; Li, Z.; Chen, J. Fabrication of antigen-containing nanoparticles using microfluidics with Tesla structure. *Electrophoresis* **2020**, *41*, 902–908. [CrossRef]
10. Sreejith, K.R.; Gorgannezhad, L.; Jin, J.; Ooi, C.H.; Stratton, H.; Dao, D.V.; Nguyen, N.-T. Liquid marbles as biochemical reactors for the polymerase chain reaction. *Lab Chip* **2019**, *19*, 3220–3227. [CrossRef]
11. Sreejith, K.R.; Gorgannezhad, L.; Jin, J.; Ooi, C.H.; Takei, T.; Hayase, G.; Stratton, H.; Lamb, K.; Shiddiky, M.; Dao, D.V.; et al. Core-Shell Beads Made by Composite Liquid Marble Technology as A Versatile Microreactor for Polymerase Chain Reaction. *Micromachines* **2020**, *11*, 242. [CrossRef] [PubMed]
12. Nguyen, N.-T.; Hejazian, M.; Ooi, C.H.; Kashaninejad, N. Recent Advances and Future Perspectives on Microfluidic Liquid Handling. *Micromachines* **2017**, *8*, 186. [CrossRef]
13. Whitesides, G.M. The origins and the future of microfluidics. *Nature* **2006**, *442*, 368–373. [CrossRef] [PubMed]
14. Nguyen, N.K.; Ooi, C.H.; Singha, P.; Jin, J.; Sreejith, K.R.; Phan, H.P.; Nguyen, N.T. Liquid Marbles as Miniature Reactors for Chemical and Biological Applications. *Processes* **2020**, *8*, 793. [CrossRef]
15. Zhang, Q.; Feng, S.; Lin, L.; Mao, S.; Lin, J.-M. Emerging open microfluidics for cell manipulation. *Chem. Soc. Rev.* **2021**, *50*, 5333–5348. [CrossRef] [PubMed]
16. Chen, M.; Shah, M.P.; Shelper, T.B.; Nazareth, L.; Barker, M.; Velasquez, J.T.; Ekberg, J.A.K.; Vial, M.-L.; John, J.A.S. Naked Liquid Marbles: A Robust Three-Dimensional Low-Volume Cell-Culturing System. *ACS Appl. Mater. Interfaces* **2019**, *11*, 9814–9823. [CrossRef] [PubMed]
17. Efremov, A.N.; Stanganello, E.; Welle, A.; Scholpp, S.; Levkin, P.A. Micropatterned superhydrophobic structures for the simultaneous culture of multiple cell types and the study of cell–cell communication. *Biomaterials* **2013**, *34*, 1757–1763. [CrossRef]

18. Song, W.; Lima, A.C.; Mano, J.F. Bioinspired methodology to fabricate hydrogel spheres for multi-applications using superhydrophobic substrates. *Soft Matter* **2010**, *6*, 5868–5871. [CrossRef]
19. Li, L.; Tian, J.; Li, M.; Shen, W. Superhydrophobic surface supported bioassay—An application in blood typing. *Colloids Surf. B Biointerfaces* **2013**, *106*, 176–180. [CrossRef]
20. Lima, A.C.; Batista, P.; Valente, T.A.; Silva, A.S.; Correia, I.J.; Mano, J.F. Novel Methodology Based on Biomimetic Superhydrophobic Substrates to Immobilize Cells and Proteins in Hydrogel Spheres for Applications in Bone Regeneration. *Tissue Eng. Part A* **2013**, *19*, 1175–1187. [CrossRef]
21. Dandan, M.; Erbil, H.Y. Evaporation Rate of Graphite Liquid Marbles: Comparison with Water Droplets. *Langmuir* **2009**, *25*, 8362–8367. [CrossRef] [PubMed]
22. Tosun, A.; Erbil, H.Y. Evaporation rate of PTFE liquid marbles. *Appl. Surf. Sci.* **2009**, *256*, 1278–1283. [CrossRef]
23. Ooi, C.H.; Vadivelu, R.; Jin, J.; Sreejith, K.R.; Singha, P.; Nguyen, N.-K.; Nguyen, N.-T. Liquid marble-based digital microfluidics—Fundamentals and applications. *Lab Chip* **2021**, *21*, 1199–1216. [CrossRef] [PubMed]
24. Polwaththe-Gallage, H.-N.; Ooi, C.H.; Jin, J.; Sauret, E.; Nguyen, N.-T.; Li, Z.; Gu, Y. The stress-strain relationship of liquid marbles under compression. *Appl. Phys. Lett.* **2019**, *114*, 043701. [CrossRef]
25. Paven, M.; Mayama, H.; Sekido, T.; Butt, H.-J.; Nakamura, Y.; Fujii, S. Light-Driven Delivery and Release of Materials Using Liquid Marbles. *Adv. Funct. Mater.* **2016**, *26*, 3199–3206. [CrossRef]
26. Chu, Y.; Liu, F.; Qin, L.; Pan, Q. Remote Manipulation of a Microdroplet in Water by Near-Infrared Laser. *ACS Appl. Mater. Interfaces* **2016**, *8*, 1273–1279. [CrossRef]
27. Ooi, C.H.; Plackowski, C.; Nguyen, A.V.; Vadivelu, R.K.; John, J.A.S.; Dao, D.V.; Nguyen, N.-T. Floating mechanism of a small liquid marble. *Sci. Rep.* **2016**, *6*, 21777. [CrossRef]
28. Yukioka, S.; Fujiwara, J.; Okada, M.; Fujii, S.; Nakamura, Y.; Yusa, S.I. CO_2-Gas-Responsive Liquid Marble. *Langmuir* **2020**, *36*, 6971–6976. [CrossRef]
29. Fernandes, A.M.; Paulis, M.; Yuan, J.; Mecerreyes, D. Magnetic Poly(Ionic Liquid) Microcapsules for Oil Capture and Recovery. *Part. Part. Syst. Charact.* **2016**, *33*, 734–739. [CrossRef]
30. Zhao, Z.; Zhang, Y.; Ren, L.; Xiang, B.; Li, J. Facile preparation of colorful liquid marbles and liquid marbles used in water pollutant detection. *J. Adhes. Sci. Technol.* **2016**, *31*, 1125–1132. [CrossRef]
31. Malinowski, R.; Parkin, I.P.; Volpe, G. Advances towards programmable droplet transport on solid surfaces and its applications. *Chem. Soc. Rev.* **2020**, *49*, 7879–7892. [CrossRef] [PubMed]
32. Bonn, D.; Eggers, J.; Indekeu, J.; Meunier, J.; Rolley, E. Wetting and spreading. *Rev. Mod. Phys.* **2009**, *81*, 739–805. [CrossRef]
33. Guo, Z.; Liu, W. Biomimic from the superhydrophobic plant leaves in nature: Binary structure and unitary structure. *Plant Sci.* **2007**, *172*, 1103–1112. [CrossRef]
34. Lu, Y.; Yu, L.; Zhang, Z.; Wu, S.; Li, G.; Wu, P.; Hu, Y.; Li, J.; Chu, J.; Wu, D. Biomimetic surfaces with anisotropic sliding wetting by energy-modulation femtosecond laser irradiation for enhanced water collection. *RSC Adv.* **2017**, *7*, 11170–11179. [CrossRef]
35. Chen, H.; Zhang, P.; Zhang, L.; Liu, H.; Jiang, Y.; Zhang, D.; Han, Z.; Jiang, L. Continuous directional water transport on the peristome surface of Nepenthes alata. *Nature* **2016**, *532*, 85–89. [CrossRef]
36. Barthlott, W.; Neinhuis, C. Purity of the sacred lotus, or escape from contamination in biological surfaces. *Planta* **1997**, *202*, 1–8. [CrossRef]
37. Öner, D.; McCarthy, T.J. Ultrahydrophobic surfaces. Effects of topography length scales on wettability. *Langmuir* **2000**, *16*, 7777–7782. [CrossRef]
38. Lei, L.; Wang, Q.; Xu, S.; Wang, N.; Zheng, X. Fabrication of superhydrophobic concrete used in marine environment with anti-corrosion and stable mechanical properties. *Constr. Build. Mater.* **2020**, *251*, 118946. [CrossRef]
39. Wang, N.; Xiong, D.; Deng, Y.; Shi, Y.; Wang, K. Mechanically Robust Superhydrophobic Steel Surface with Anti-Icing, UV-Durability, and Corrosion Resistance Properties. *ACS Appl. Mater. Interfaces* **2015**, *7*, 6260–6272. [CrossRef]
40. Han, H.; Lee, J.S.; Kim, H.; Shin, S.; Lee, J.; Kim, J.; Hou, X.; Cho, S.W.; Seo, J.; Lee, T. Single-Droplet Multiplex Bioassay on a Robust and Stretchable Extreme Wetting Substrate through Vacuum-Based Droplet Manipulation. *ACS Nano* **2018**, *12*, 932–941. [CrossRef]
41. Gross, M.; Varnik, F.; Raabe, D.; Steinbach, I. Small droplets on superhydrophobic substrates. *Phys. Rev. E* **2010**, *81*, 051606. [CrossRef] [PubMed]
42. Wenzel, R.N. Resistance of solid surfaces to wetting by water. *Ind. Eng. Chem.* **1936**, *28*, 988–994. [CrossRef]
43. Cassie, A.B.D.; Baxter, S. Wettability of porous surfaces. *Trans. Faraday Soc.* **1944**, *40*, 546–551. [CrossRef]
44. Kasahara, M.; Akimoto, S.-I.; Hariyama, T.; Takaku, Y.; Yusa, S.-I.; Okada, S.; Nakajima, K.; Hirai, T.; Mayama, H.; Okada, S.; et al. Liquid Marbles in Nature: Craft of Aphids for Survival. *Langmuir* **2019**, *35*, 6169–6178. [CrossRef]
45. Aussillous, P.; Quéré, D. Liquid marbles. *Nature* **2001**, *411*, 924–927. [CrossRef]
46. Oliveira, N.M.; Zhang, Y.S.; Ju, J.; Chen, A.-Z.; Chen, Y.; Sonkusale, S.R.; Dokmeci, M.R.; Reis, R.L.; Mano, J.F.; Khademhosseini, A. Hydrophobic Hydrogels: Toward Construction of Floating (Bio)microdevices. *Chem. Mater.* **2016**, *28*, 3641–3648. [CrossRef]
47. Pennarossa, G.; Manzoni, E.F.M.; Ledda, S.; Deeguileor, M.; Gandolfi, F.; Brevini, T.A.L. Use of a PTFE Micro-Bioreactor to Promote 3D Cell Rearrangement and Maintain High Plasticity in Epigenetically Erased Fibroblasts. *Stem Cell Rev. Rep.* **2018**, *15*, 82–92. [CrossRef] [PubMed]

48. Tian, J.; Fu, N.; Chen, X.D.; Shen, W. Respirable liquid marble for the cultivation of microorganisms. *Colloids Surf. B Biointerfaces* **2013**, *106*, 187–190. [CrossRef]
49. Vadivelu, R.K.; Ooi, C.H.; Yao, R.-Q.; Velasquez, J.T.; Pastrana, E.; Diaz-Nido, J.; Lim, F.; Ekberg, J.A.K.; Nguyen, N.-T.; John, J.A.S. Generation of three-dimensional multiple spheroid model of olfactory ensheathing cells using floating liquid marbles. *Sci. Rep.* **2015**, *5*, 15083. [CrossRef]
50. Sreejith, K.R.; Ooi, C.H.; Dao, D.V.; Nguyen, N.-T. Evaporation dynamics of liquid marbles at elevated temperatures. *RSC Adv.* **2018**, *8*, 15436–15443. [CrossRef]
51. McHale, G.; Newton, M.I. Liquid marbles: Principles and applications. *Soft Matter* **2011**, *7*, 5473–5481. [CrossRef]
52. Saczek, J.; Yao, X.; Zivkovic, V.; Mamlouk, M.; Wang, D.; Pramana, S.S.; Wang, S. Long-Lived Liquid Marbles for Green Applications. *Adv. Funct. Mater.* **2021**, *31*, 2011198. [CrossRef]
53. Zang, D.; Chen, Z.; Zhang, Y.; Lin, K.; Geng, X.; Binks, B.P. Effect of particle hydrophobicity on the properties of liquid water marbles. *Soft Matter* **2013**, *9*, 5067–5073. [CrossRef]
54. Dickinson, E.; Ettelaie, R.; Kostakis, T.; Murray, B.S. Factors Controlling the Formation and Stability of Air Bubbles Stabilized by Partially Hydrophobic Silica Nanoparticles. *Langmuir* **2004**, *20*, 8517–8525. [CrossRef]
55. Cengiz, U.; Erbil, H.Y. The lifetime of floating liquid marbles: The influence of particle size and effective surface tension. *Soft Matter* **2013**, *9*, 8980–8991. [CrossRef]
56. Liu, Z.; Zhang, Y.; Chen, C.; Yang, T.; Wang, J.; Guo, L.; Liu, P.; Kong, T. Larger Stabilizing Particles Make Stronger Liquid Marble. *Small* **2018**, *15*, e1804549. [CrossRef]
57. Fullarton, C.; Draper, T.C.; Phillips, N.; Mayne, R.; Costello, B.P.J.D.L.; Adamatzky, A. Evaporation, Lifetime, and Robustness Studies of Liquid Marbles for Collision-Based Computing. *Langmuir* **2018**, *34*, 2573–2580. [CrossRef]
58. Nguyen, T.H.; Hapgood, K.; Shen, W. Observation of the liquid marble morphology using confocal microscopy. *Chem. Eng. J.* **2010**, *162*, 396–405. [CrossRef]
59. Asaumi, Y.; Rey, M.; Oyama, K.; Vogel, N.; Hirai, T.; Nakamura, Y.; Fujii, S. Effect of Stabilizing Particle Size on the Structure and Properties of Liquid Marbles. *Langmuir* **2020**, *36*, 13274–13284. [CrossRef]
60. Singha, P.; Nguyen, N.K.; Nguyen, V.T.; Sreejith, K.R.; Tran, D.T.; Nguyen, A.V.; Nguyen, N.T.; Ooi, C.H. Investigation of liquid marble shell using X-ray: Shell thickness and effective surface tension. *ChemNanoMat* **2021**, *8*, e202100423. [CrossRef]
61. Huang, J.; Wang, Z.; Shi, H.; Li, X. Mechanical robustness of monolayer nanoparticle-covered liquid marbles. *Soft Matter* **2020**, *16*, 4632–4639. [CrossRef] [PubMed]
62. Li, X.; Shi, H.; Wang, Y.; Wang, H.; Huang, J.; Duan, M. Liquid marbles from soot films. *Soft Matter* **2020**, *16*, 4512–4519. [CrossRef] [PubMed]
63. Laborie, B.; Lachaussée, F.; Lorenceau, E.; Rouyer, F. How coatings with hydrophobic particles may change the drying of water droplets: Incompressible surface versus porous media effects. *Soft Matter* **2013**, *9*, 4822–4830. [CrossRef]
64. Gao, N.; Geyer, F.; Pilat, D.W.; Wooh, S.; Vollmer, D.; Butt, H.-J.; Berger, R. How drops start sliding over solid surfaces. *Nat. Phys.* **2017**, *14*, 191–196. [CrossRef]
65. Mahadevan, L.; Pomeau, Y. Rolling droplets. *Phys. Fluids* **1999**, *11*, 2449–2453. [CrossRef]
66. Olin, P.; Lindström, S.B.; Pettersson, T.; Wågberg, L. Water Drop Friction on Superhydrophobic Surfaces. *Langmuir* **2013**, *29*, 9079–9089. [CrossRef]
67. Backholm, M.; Molpeceres, D.; Vuckovac, M.; Nurmi, H.; Hokkanen, M.J.; Jokinen, V.; Timonen, J.V.I.; Ras, R.H.A. Water droplet friction and rolling dynamics on superhydrophobic surfaces. *Commun. Mater.* **2020**, *1*, 1–8. [CrossRef]
68. Extrand, C.W.; Kumagai, Y. Liquid Drops on an Inclined Plane: The Relation between Contact Angles, Drop Shape, and Retentive Force. *J. Colloid Interface Sci.* **1995**, *170*, 515–521. [CrossRef]
69. Bormashenko, E.; Bormashenko, Y.; Oleg, G. On the Nature of the Friction between Nonstick Droplets and Solid Substrates. *Langmuir* **2010**, *26*, 12479–12482. [CrossRef]
70. Aussillous, P.; Quéré, D. Properties of liquid marbles. *Proc. R. Soc. A Math. Phys. Eng. Sci.* **2006**, *462*, 973–999. [CrossRef]
71. Ooi, C.H.; Jin, J.; Sreejith, K.R.; Nguyen, A.V.; Evans, G.M.; Nguyen, N.-T. Manipulation of a floating liquid marble using dielectrophoresis. *Lab Chip* **2018**, *18*, 3770–3779. [CrossRef] [PubMed]
72. Ooi, C.H.; Nguyen, A.V.; Evans, G.M.; Dao, D.V.; Nguyen, N.T. Measuring the Coefficient of Friction of a Small Floating Liquid Marble. *Sci. Rep.* **2016**, *6*, 38346. [CrossRef] [PubMed]
73. Brochard, F. Motions of droplets on solid surfaces induced by chemical or thermal gradients. *Langmuir* **1989**, *5*, 432–438. [CrossRef]
74. Shastry, A.; Case, M.J.; Böhringer, K.F. Directing Droplets Using Microstructured Surfaces. *Langmuir* **2006**, *22*, 6161–6167. [CrossRef] [PubMed]
75. Berge, B. Electrocapillarity and wetting of insulator films by water. *Comptes Rendus De L Acad. Des Sci. Ser. Ii* **1993**, *317*, 157–163.
76. Mugele, F.; Baret, J.-C. Electrowetting: From basics to applications. *J. Phys. Condens. Matter* **2005**, *17*, R705–R774. [CrossRef]
77. Newton, M.I.; Herbertson, D.L.; Elliott, S.J.; Shirtcliffe, N.J.; McHale, G. Electrowetting of liquid marbles. *J. Phys. D Appl. Phys.* **2007**, *40*, 20–24. [CrossRef]
78. Baird, E.; Young, P.; Mohseni, K. Electrostatic force calculation for an EWOD-actuated droplet. *Microfluid. Nanofluidics* **2007**, *3*, 635–644. [CrossRef]
79. Barman, J.; Shao, W.; Tang, B.; Yuan, D.; Groenewold, J.; Zhou, G. Wettability Manipulation by Interface-Localized Liquid Dielectrophoresis: Fundamentals and Applications. *Micromachines* **2019**, *10*, 329. [CrossRef]

80. Pethig, R. Review article-dielectrophoresis: Status of the theory, technology, and applications. *Biomicrofluidics* **2010**, *4*, 022811. [CrossRef]
81. Long, Z.; Shetty, A.M.; Solomon, M.; Larson, R.G. Fundamentals of magnet-actuated droplet manipulation on an open hydrophobic surface. *Lab Chip* **2009**, *9*, 1567–1575. [CrossRef] [PubMed]
82. Friend, J.; Yeo, L.Y. Microscale acoustofluidics: Microfluidics driven via acoustics and ultrasonics. *Rev. Mod. Phys.* **2011**, *83*, 647–704. [CrossRef]
83. Sudeepthi, A.; Nath, A.; Yeo, L.Y.; Sen, A.K. Coalescence of Droplets in a Microwell Driven by Surface Acoustic Waves. *Langmuir* **2021**, *37*, 1578–1587. [CrossRef]
84. Andrade, M.A.B.; Camargo, T.S.A.; Marzo, A. Automatic contactless injection, transportation, merging, and ejection of droplets with a multifocal point acoustic levitator. *Rev. Sci. Instrum.* **2018**, *89*, 125105. [CrossRef] [PubMed]
85. Ai, Y.; Marrone, B.L. Droplet translocation by focused surface acoustic waves. *Microfluid. Nanofluidics* **2012**, *13*, 715–722. [CrossRef]
86. Yeo, L.Y.; Friend, J.R. Surface Acoustic Wave Microfluidics. *Annu. Rev. Fluid Mech.* **2014**, *46*, 379–406. [CrossRef]
87. Li, J.; Guo, Z. Spontaneous directional transportations of water droplets on surfaces driven by gradient structures. *Nanoscale* **2018**, *10*, 13814–13831. [CrossRef]
88. Brzoska, J.B.; Brochard-Wyart, F.; Rondelez, F. Motions of droplets on hydrophobic model surfaces induced by thermal gradients. *Langmuir* **1993**, *9*, 2220–2224. [CrossRef]
89. Cira, N.J.; Benusiglio, A.; Prakash, M. Vapour-mediated sensing and motility in two-component droplets. *Nature* **2015**, *519*, 446–450. [CrossRef]
90. Bormashenko, E.; Bormashenko, Y.; Grynyov, R.; Aharoni, H.; Whyman, G.; Binks, B.P. Self-Propulsion of Liquid Marbles: Leidenfrost-like Levitation Driven by Marangoni Flow. *J. Phys. Chem. C* **2015**, *119*, 9910–9915. [CrossRef]
91. Higuera, F.J.; Medina, A.; Liñán, A. Capillary rise of a liquid between two vertical plates making a small angle. *Phys. Fluids* **2008**, *20*, 102102. [CrossRef]
92. Ju, J.; Xiao, K.; Yao, X.; Bai, H.; Jiang, L. Bioinspired Conical Copper Wire with Gradient Wettability for Continuous and Efficient Fog Collection. *Adv. Mater.* **2013**, *25*, 5937–5942. [CrossRef]
93. Alosaimi, F.K.; Tung, T.T.; Dao, V.-D.; Huyen, N.K.; Nine, J.; Hassan, K.; Ma, J.; Losic, D. Graphene-based multifunctional surface and structure gradients engineered by atmospheric plasma. *Appl. Mater. Today* **2022**, *27*, 101486. [CrossRef]
94. Hernández, S.C.; Bennett, C.J.C.; Junkermeier, C.; Tsoi, S.D.; Bezares, F.J.; Stine, R.; Robinson, J.; Lock, E.; Boris, D.R.; Pate, B.D.; et al. Chemical Gradients on Graphene to Drive Droplet Motion. *ACS Nano* **2013**, *7*, 4746–4755. [CrossRef] [PubMed]
95. Li, Y.; Huang, J.; Cheng, J.; Xu, S.; Pi, P.; Wen, X. Enhanced Movement of Two-Component Droplets on a Wedge-Shaped Ag/Cu Surface by a Wettability Gradient. *ACS Appl. Mater. Interfaces* **2021**, *13*, 15857–15865. [CrossRef]
96. Aliabadi, M.; Zarkesh, A.; Siampour, H.; Abbasian, S.; Mahdavinejad, M.; Moshaii, A. Bioinspired Azimuthally Varying Nanoscale Cu Columns on Acupuncture Needles for Fog Collection. *ACS Appl. Nano Mater.* **2021**, *4*, 8733–8743. [CrossRef]
97. Bormashenko, E.; Pogreb, R.; Whyman, G.; Musin, A. Jetting liquid marbles: Study of the Taylor instability in immersed marbles. *Colloid Polym. Sci.* **2013**, *291*, 1535–1539. [CrossRef]
98. McHale, G.; Herbertson, D.L.; Elliott, S.J.; Shirtcliffe, N.J.; Newton, M.I. Electrowetting of Nonwetting Liquids and Liquid Marbles. *Langmuir* **2006**, *23*, 918–924. [CrossRef]
99. Khaw, M.K.; Ooi, C.H.; Mohd-Yasin, F.; Vadivelu, R.; John, J.S.; Nguyen, N.-T. Digital microfluidics with a magnetically actuated floating liquid marble. *Lab Chip* **2016**, *16*, 2211–2218. [CrossRef]
100. Li, A.; Li, H.; Li, Z.; Zhao, Z.; Li, K.; Li, M.; Song, Y. Programmable droplet manipulation by a magnetic-actuated robot. *Sci. Adv.* **2020**, *6*, eaay5808. [CrossRef]
101. Timonen, J.V.I.; Latikka, M.; Leibler, L.; Ras, R.H.A.; Ikkala, O. Switchable Static and Dynamic Self-Assembly of Magnetic Droplets on Superhydrophobic Surfaces. *Science* **2013**, *341*, 253–257. [CrossRef] [PubMed]
102. Wixforth, A.; Strobl, C.; Gauer, C.; Toegl, A.; Scriba, J.; von Guttenberg, Z. Acoustic manipulation of small droplets. *Anal. Bioanal. Chem.* **2004**, *379*, 982–991. [CrossRef]
103. Diguet, A.; Guillermic, R.-M.; Magome, N.; Saint-Jalmes, A.; Chen, Y.; Yoshikawa, K.; Baigl, D. Photomanipulation of a Droplet by the Chromocapillary Effect. *Angew. Chem. Int. Ed.* **2009**, *48*, 9281–9284. [CrossRef]
104. Greenspan, H.P. On the motion of a small viscous droplet that wets a surface. *J. Fluid Mech.* **1978**, *84*, 125. [CrossRef]
105. Chaudhury, M.K.; Whitesides, G.M. How to Make Water Run Uphill. *Science* **1992**, *256*, 1539–1541. [CrossRef] [PubMed]
106. van Assenbergh, P.; Meinders, E.; Geraedts, J.; Dodou, D. Nanostructure and Microstructure Fabrication: From Desired Properties to Suitable Processes. *Small* **2018**, *14*, e1703401. [CrossRef] [PubMed]
107. Zheng, Y.; Cheng, J.; Zhou, C.; Xing, H.; Wen, X.; Pi, P.; Xu, S. Droplet Motion on a Shape Gradient Surface. *Langmuir* **2017**, *33*, 4172–4177. [CrossRef]
108. Han, X.; Wang, L.; Wang, X. Fabrication of Chemical Gradient Using Space Limited Plasma Oxidation and its Application for Droplet Motion. *Adv. Funct. Mater.* **2012**, *22*, 4533–4538. [CrossRef]
109. Washizu, M. Electrostatic actuation of liquid droplets for micro-reactor applications. *IEEE Trans. Ind. Appl.* **1998**, *34*, 732–737. [CrossRef]
110. Bormashenko, E.; Pogreb, R.; Balter, R.; Gendelman, O.; Aurbach, D. Composite non-stick droplets and their actuation with electric field. *Appl. Phys. Lett.* **2012**, *100*, 151601. [CrossRef]

111. Ooi, C.H.; Jin, J.; Nguyen, A.V.; Evans, G.M.; Nguyen, N.-T. Picking up and placing a liquid marble using dielectrophoresis. *Microfluid. Nanofluidics* **2018**, *22*, 142. [CrossRef]
112. Jin, J.; Ooi, C.H.; Sreejith, K.R.; Dao, D.V.; Nguyen, N.-T. Dielectrophoretic Trapping of a Floating Liquid Marble. *Phys. Rev. Appl.* **2019**, *11*, 044059. [CrossRef]
113. Jin, J.; Ooi, C.H.; Sreejith, K.R.; Zhang, J.; Nguyen, A.V.; Evans, G.M.; Dao, D.V.; Nguyen, N.-T. Accurate dielectrophoretic positioning of a floating liquid marble with a two-electrode configuration. *Microfluid. Nanofluidics* **2019**, *23*, 85. [CrossRef]
114. Lee, J.; Moon, H.; Fowler, J.; Schoellhammer, T.; Kim, C.-J. Electrowetting and electrowetting-on-dielectric for microscale liquid handling. *Sens. Actuators A Phys.* **2002**, *95*, 259–268. [CrossRef]
115. Cooney, C.G.; Chen, C.-Y.; Emerling, M.R.; Nadim, A.; Sterling, J.D. Electrowetting droplet microfluidics on a single planar surface. *Microfluid. Nanofluidics* **2006**, *2*, 435–446. [CrossRef]
116. Zhang, Y.; Wang, T.-H. Full-Range Magnetic Manipulation of Droplets via Surface Energy Traps Enables Complex Bioassays. *Adv. Mater.* **2013**, *25*, 2903–2908. [CrossRef]
117. Yang, C.; Ning, Y.; Ku, X.; Zhuang, G.; Li, G. Automatic magnetic manipulation of droplets on an open surface using a superhydrophobic electromagnet needle. *Sens. Actuators B Chem.* **2018**, *257*, 409–418. [CrossRef]
118. Damodara, S.; Sen, A. Magnetic field assisted droplet manipulation on a soot-wax coated superhydrophobic surface of a PDMS-iron particle composite substrate. *Sens. Actuators B Chem.* **2017**, *239*, 816–823. [CrossRef]
119. Yang, C.; Zhang, Z.; Li, G. Programmable droplet manipulation by combining a superhydrophobic magnetic film and an electromagnetic pillar array. *Sens. Actuators B Chem.* **2018**, *262*, 892–901. [CrossRef]
120. Fan, X.; Dong, X.; Karacakol, A.C.; Xie, H.; Sitti, M. Reconfigurable multifunctional ferrofluid droplet robots. *Proc. Natl. Acad. Sci. USA* **2020**, *117*, 27916–27926. [CrossRef]
121. Zhao, Y.; Fang, J.; Wang, H.; Wang, X.; Lin, T. Magnetic liquid marbles: Manipulation of liquid droplets using highly hydrophobic Fe_3O_4 nanoparticles. *Adv. Mater.* **2010**, *22*, 707–710. [CrossRef] [PubMed]
122. Xue, Y.; Wang, H.; Zhao, Y.; Dai, L.; Feng, L.; Wang, X.; Lin, T. Magnetic liquid marbles: A "precise" miniature reactor. *Adv. Mater.* **2010**, *22*, 4814–4818. [CrossRef] [PubMed]
123. Vialetto, J.; Hayakawa, M.; Kavokine, N.; Takinoue, M.; Varanakkottu, S.N.; Rudiuk, S.; Anyfantakis, M.; Morel, M.; Baigl, D. Magnetic Actuation of Drops and Liquid Marbles Using a Deformable Paramagnetic Liquid Substrate. *Angew. Chem. Int. Ed.* **2017**, *56*, 16565–16570. [CrossRef] [PubMed]
124. Bourquin, Y.; Reboud, J.; Wilson, R.; Cooper, J.M. Tuneable surface acoustic waves for fluid and particle manipulations on disposable chips. *Lab Chip* **2010**, *10*, 1898–1901. [CrossRef]
125. Yang, T.-H.; Yang, H.-C.; Chang, C.-H.; Prabhu, G.R.D.; Urban, P.L. Microanalysis Using Acoustically Actuated Droplets Pinned Onto a Thread. *IEEE Access* **2019**, *7*, 154743–154749. [CrossRef]
126. Zang, D.; Li, J.; Chen, Z.; Zhai, Z.; Geng, X.; Binks, B.P. Switchable Opening and Closing of a Liquid Marble via Ultrasonic Levitation. *Langmuir* **2015**, *31*, 11502–11507. [CrossRef]
127. Chen, Z.; Zang, D.; Zhao, L.; Qu, M.; Li, X.; Li, X.; Li, L.; Geng, X. Liquid Marble Coalescence and Triggered Microreaction Driven by Acoustic Levitation. *Langmuir* **2017**, *33*, 6232–6239. [CrossRef]
128. Ichimura, K.; Oh, S.-K.; Nakagawa, M. Light-Driven Motion of Liquids on a Photoresponsive Surface. *Science* **2000**, *288*, 1624–1626. [CrossRef]
129. Hwang, H.; Papadopoulos, P.; Fujii, S.; Wooh, S. Driving Droplets on Liquid Repellent Surfaces via Light-Driven Marangoni Propulsion. *Adv. Funct. Mater.* **2022**, *32*, 2111311. [CrossRef]
130. Kavokine, N.; Anyfantakis, M.; Morel, M.; Rudiuk, S.; Bickel, T.; Baigl, D. Light-Driven Transport of a Liquid Marble with and against Surface Flows. *Angew. Chem. Int. Ed.* **2016**, *55*, 11183–11187. [CrossRef]
131. Jin, J.; Ooi, C.H.; Dao, D.V.; Nguyen, N.-T. Coalescence Processes of Droplets and Liquid Marbles. *Micromachines* **2017**, *8*, 336. [CrossRef] [PubMed]
132. Paulsen, J.D.; Burton, J.C.; Nagel, S.R.; Appathurai, S.; Harris, M.T.; Basaran, O.A. The inexorable resistance of inertia determines the initial regime of drop coalescence. *Proc. Natl. Acad. Sci. USA* **2012**, *109*, 6857–6861. [CrossRef] [PubMed]
133. Liu, Z.; Fu, X.; Binks, B.P.; Shum, H.C. Coalescence of electrically charged liquid marbles. *Soft Matter* **2016**, *13*, 119–124. [CrossRef]
134. Jin, J.; Ooi, C.H.; Dao, D.V.; Nguyen, N.-T. Liquid marble coalescence via vertical collision. *Soft Matter* **2018**, *14*, 4160–4168. [CrossRef] [PubMed]
135. Rozynek, Z.; Khobaib, K.; Mikkelsen, A. Opening and Closing of Particle Shells on Droplets via Electric Fields and Its Applications. *ACS Appl. Mater. Interfaces* **2019**, *11*, 22840–22850. [CrossRef]
136. Nguyen, N.K.; Singha, P.; An, H.; Phan, H.P.; Nguyen, N.T.; Ooi, C.H. Electrostatically excited liquid marble as a micromixer. *React. Chem. Eng.* **2021**, *6*, 1386–1394. [CrossRef]
137. Nguyen, N.K.; Singha, P.; Dai, Y.; Sreejith, K.R.; Phan, H.P.; Nguyen, N.T.; Ooi, C.H. Controllable high-performance liquid marble micromixer. *Lab Chip* **2022**, *22*, 1508–1518. [CrossRef]
138. Wang, E.N.; Bucaro, M.A.; Taylor, J.A.; Kolodner, P.; Aizenberg, J.; Krupenkin, T. Droplet mixing using electrically tunable superhydrophobic nanostructured surfaces. *Microfluid. Nanofluidics* **2008**, *7*, 137–140. [CrossRef]
139. Won, T.; Lee, K.Y.; Chung, S.K. *Proceedings of the 2019 20th International Conference on Solid-State Sensors, Actuators and Microsystems & Eurosensors XXXIII (TRANSDUCERS & EUROSENSORS XXXIII), Berlin, Germany, 23–27 June 2019*; IEEE: Manhattan, NY, USA, 2019; pp. 65–67.

140. Liu, Z.; Yang, T.; Huang, Y.; Liu, Y.; Chen, L.; Deng, L.; Shum, H.C.; Kong, T. Electrocontrolled Liquid Marbles for Rapid Miniaturized Organic Reactions. *Adv. Funct. Mater.* **2019**, *29*, 1901101. [CrossRef]
141. Pollack, M.G.; Shenderov, A.D.; Fair, R.B. Electrowetting-based actuation of droplets for integrated microfluidics. *Lab Chip* **2002**, *2*, 96–101. [CrossRef]
142. Mertaniemi, H.; Jokinen, V.; Sainiemi, L.; Franssila, S.; Marmur, A.; Ikkala, O.; Ras, R.H.A. Superhydrophobic Tracks for Low-Friction, Guided Transport of Water Droplets. *Adv. Mater.* **2011**, *23*, 2911–2914. [CrossRef] [PubMed]
143. Song, D.; Song, B.; Hu, H.; Du, X.; Zhou, F. Selectively splitting a droplet using superhydrophobic stripes on hydrophilic surfaces. *Phys. Chem. Chem. Phys.* **2015**, *17*, 13800–13803. [CrossRef] [PubMed]
144. Wang, B.; Chan, K.F.; Ji, F.; Wang, Q.; Chiu, P.W.Y.; Guo, Z.; Zhang, L. On-Demand Coalescence and Splitting of Liquid Marbles and Their Bioapplications. *Adv. Sci.* **2019**, *6*, 1802033. [CrossRef]
145. Liu, J.; Zuo, P. Wetting and elasto-plasticity based sculpture of liquid marbles. *Eur. Phys. J. E* **2016**, *39*, 17. [CrossRef] [PubMed]
146. Yang, Y.; Chen, R.; Zhu, X.; Ye, D.; Yang, Y.; Li, W.; Li, D.; Li, H.; Liao, Q. Micro-object manipulation by decanol liquid lenses. *Lab Chip* **2022**, *22*, 2844–2852. [CrossRef] [PubMed]